Characterization of global gene expression after S100A4 mRNA transfection

Agnethe Sandvik Ouren

Thesis for the Master's degree in Molecular Biosciences

60 study points

UNIVERSITY OF OSLO

Department of Molecular Biosciences

Faculty of Mathematics and Natural Sciences

May 2011

Abstract

Gene therapy strategies have been intensively studied for over 20 years. However, there are yet no gene therapy protocols in conventional use. In this project, a gene delivery protocol was optimized for the transient delivery of mRNA molecules into two human cancer cell lines with the purpose of disclosing novel S100A4 gene interactions as a result of S100A4 overexpression.

The Enhanced Green Fluorescent Protein (EGFP) and the metastasis-promoting S100A4 gene were used in this study. To deliver mRNA molecules we investigated the potential of two different delivery vehicles, the bio-compatible transfection carrier β-cyclodextrin and the well characterized polyethylenimine (PEI) carrier. In addition, we evaluated the possibility for targeted mRNA delivery by the use of photochemical internalization (PCI) technology, a site-specific delivery strategy. Our results showed that PEI was an effective carrier for delivery of mRNA either with or without PCI, which was in contrast to β-cyclodextrin.

To evaluate potential novel S100A4 gene interactions we preformed microarray profiling of two S100A4 mRNA overexpressing cell lines (OHS and LOX). Some of the most affected genes were chosen for reverse transcriptase quantitative PCR verification. The transporter lipocalin 12 and the collagen precursor Col1a2 were confirmed to be affected by S100A4 overexpression.

Acknowledgements

This thesis concludes my Masters degree in Molecular Bioscience at the Department of Molecular Biosciences (IMBV) at the University of Oslo. The study was carried out at the Norwegian Radium Hospital in the group of Eivind Hovig.

My sincere thanks go to my advisor Sigurd Leinæs Bøe, for many hours of patient assistance and encouragement throughout the project, as well as Eivind Hovig for making me a part of his research group, challenging me, and immediately seeing solutions to problems I could have been struggling with for days. This group is a truly great working environment, and I am humbled to work with such brilliant people. I would also like to thank the rest of the Gene Therapy group, especially Ane Sager Longva for patient help in the lab, and Jens Andreas Lindin Jørgensen for collaboration throughout (and a memorable Winter Meeting in Tromsø). Thank you Ingrid Johanne Bettum for insistent encouragement and practical advice, and Vegard Nygaard of the Microarray facility for help interpreting my results. My internal advisor Ola Myklebost also deserves thanks for making the arrangements to make this project possible.

My family has been a dependable source of support and encouragement throughout these two years. Thank you for everything you continue to do for me and others. And finally; Thank you Øyvind for always believing in me and making me feel like I can accomplish anything.

Contents

8

1. Introduction

1.1 Cancer

Cancer is a generic term describing a large group of conditions caused by uncontrolled cell growth within the body, and is also referred to as malignant tumors or neoplasms. Cancer takes its name from the Greek word for crab, *karkinos,* due to the crab-like projections seen in some malignant tumors. [1]

1.1.1 Relevance of studying cancer

Cancer beats ischaemic heart disease as the number one cause of death in the developed world according to World Health Organization reports, accounting for one in eight deaths worldwide. [2, 3] Since American President Richard Nixon essentially gave the cancer research community *carte blanche* in the 1971 Cancer Act, [4] an enormous effort has been put into cancer research and treatment. Still, cancer incidence continues to rise internationally, even when correcting for population growth, and especially in developing countries. This is partly due to increased life expectancies and improved methods of diagnosis. [2] The need for a continued effort to work out the molecular causes of the condition is evident.

Studying cancer can also give a greater understanding of healthy biology. By detecting the genetic and epigenetic changes in a cancer and observing their effects on the functions of the cell, insights about the normal function of the genes can be derived.

1.1.2 Cancer as a microevolutionary process

Cells in a multicellular organism are tightly controlled to act as constituents of a whole, and will normally never divide unless stimulated by their environment to do

so. Cancerous cells behave more like single celled organisms; dividing as much as the available resources allow. This loss of top-down control arises from random mutations in the genomes of individual cells. Active, metabolizing human cells are continuously subject to DNA damage, estimated to ~800 lesions per cell per hour. [5] The vast majority of the damages are rapidly reverted by efficient DNA repair systems, but those that are not repaired correctly stay in the genome as mutations (alterations of the DNA sequence). Mutations accumulate over time and are preserved in subsequent cell divisions. This is the main reason why cancers most often occur in old age. [6] Cancer-promoting mutations can be divided into two groups: those that cause loss of function or down-regulation of tumor suppressor genes, and those that enhance expression or function of proto-oncogenes. Additionally, mutations that impair the DNA repair machinery or epigenetic mark-up of DNA facilitate cancer progression by promoting further genetic damage and dysregulation.

Due to redundancy and backup mechanisms, no single mutation can cause cancer alone, but multiple mutations in vital genes put the cell at risk of evading the normal restrictions on proliferation. [6, 7]

A set of phenotypical properties necessary for cancer development termed the hallmarks of cancer were posted by Hanahan and Weinberg in 2000; self-sufficiency in growth signals, insensitivity to growth-inhibitory signals, evasion of apoptosis (programmed cell death), limitless replicative potential, sustained angiogenesis, and tissue invasion and metastasis. Mutations promoting one (or multiple) of these hallmarks make the cell more likely to persist, survive, and divide uncontrolled. [8] The hallmarks are illustrated in figure 1.1.
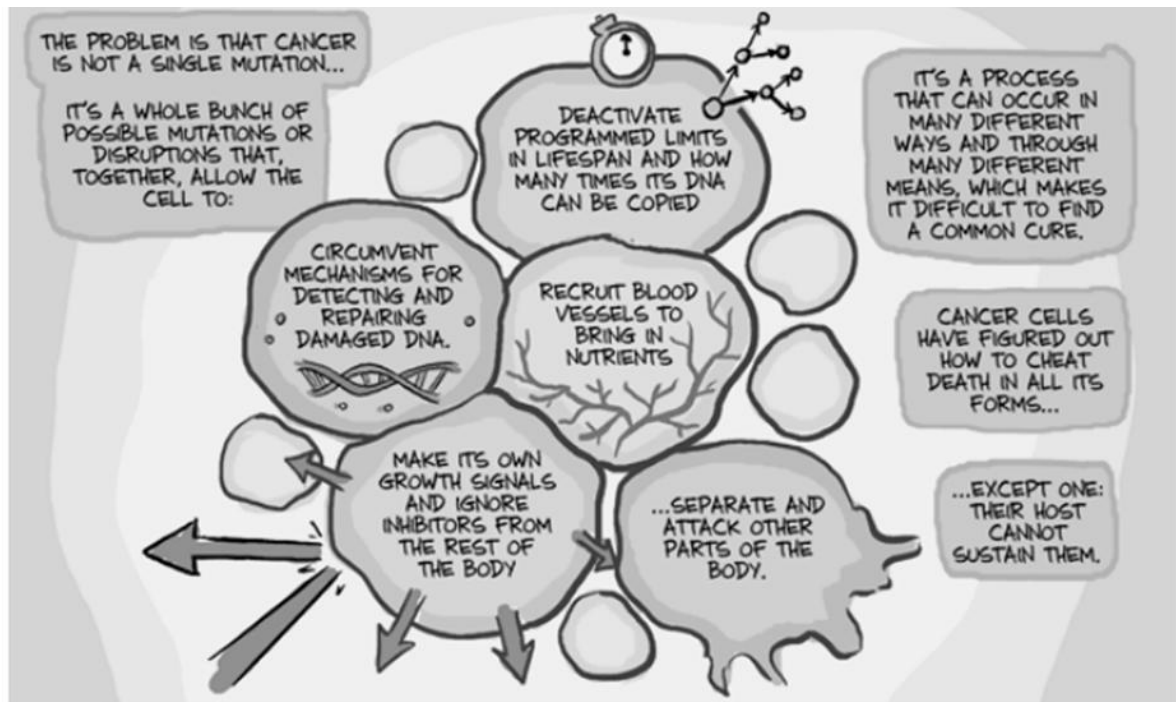
Figure 1.1: The cancer hallmarks. phdcomics.com, used with permission.

The complexity of cancer genetics is immense; no two cancer cases have the same genetic profile. Still, some mutations are frequently found in cancers. What these mutations have in common is giving the affected cell a selective advantage in the environment that is our body.

1.1.3 Changes in gene expression in cancer

The human genome contains more than 20 000 genes, of which roughly half are expressed in all cells at all times (these are called household genes), and the rest are specific to certain tissues or cell types, or expressed only in response to certain stimuli. Any one cell expresses less than a thousand specific genes, which give them their defining traits. [9] The rest of the genome is locked away by epigenetic packing, mainly DNA methylation. [10]

When a gene is expressed, it is transcribed to mRNA in the nucleus, complexed with chaperone proteins and transported out into the cytoplasm where it is translated to

protein by ribosomes. All steps in this process are subject to regulation (see [6] p 415).

As all cells contain the entire genome, any cell may by accident gain access to genetic information that is normally not accessible to them. When this happens in genes that take part in the tight regulation of cell fate, control mechanisms may be compromised. Such changes may occur through a decrease in DNA methylation, mutations in the regulatory elements that keep the gene turned off, or chromosomal rearrangements that put the gene in a close proximity to a strong promoter sequence. Conversely, tumor suppressor genes are often observed to be down-regulated in cancer. [10]

1.2 Gene therapy

Genetic diseases are caused by mutated or otherwise malfunctioning genes. Gene therapy seeks to correct genetic diseases by inserting normal copies of the gene into cells, or remove the expression of the erroneous gene. The experimental insertion of genetic material (DNA or RNA) into cultured cells is called transfection (*trans* - from the outside). Vectors that can be used for transfection include engineered viruses, ribozymes, locked RNA (LNA), and peptide nucleic acids (PNA). Gene therapy has been proposed as treatment for a wide range of conditions including cystic fibrosis, [11] Parkinson's disease, [12] Huntington's disease, [13] severe combined immunodeficiency (SCID; [14]) and cancer. [15], [16]

After 20 years and over 1500 clinical trials, gene therapy is yet to be implemented in the clinic, with the notable exception of immunotherapy using transfected immune cells. [17] The main problems have been the controlled and safe integration of DNA into the genome, adverse immune responses against the transfection agent or the transgene, in addition to cytotoxicity (cell death caused by the transfection itself or the overexpressed gene). [18]

1.2.1 Gene therapy in cancer

As cancer is a genetic disease, the notion of correcting it with gene therapy is compelling. However, despite tremendous efforts over many years, these approaches are still experimental. As mentioned in section 1.1, cancer is caused by a range of defects acting in concert, and differently in every single patient. By reverting some, but not all of the changes in the cancerous cell, the cancer could become more likely to evade apoptosis, thereby becoming more severe. Also, unlike hereditary genetic diseases in which the genetic defect is present in all cells, a cancer is surrounded by normal tissue that preferably should be untreated to avoid off-target effects. A site-directed delivery method for gene therapy is therefore preferable to target the cancerous cells.

1.2.2 Transfection agents

Two cationic transfection agents were used in the study, alone and in combination with light-directed endosomal rupture (PCI).

Polyethylenimine

The organic, polycationic polymer polyethylenimine (PEI; $H(NHCH_2CH_2)_nNH_2$) is a cost-efficient excipient (carrier) for *in vitro* transfection. [19, 20] It may, however, be less suited for *in vivo* applications due to reported cytotoxic effects of compromising the integrity of the plasma membrane[21] and mitochondria membranes. [22] 25 kDa branched PEI was selected, on the basis of being well characterized and known to produce high transfection rates when combined with either siRNA or mRNA molecules. [23, 24]

When using this carrier, the charge of the transfection complex is essential for uptake into cells. The theoretical charge is calculated from the ratio between **N**itrogen and **P**hosphate (N/P) in the complex, as these are the charge-bearing elements present in

the compounds. At neutral pH, all phosphate groups on mRNA bear a negative charge, while around one in three amine groups on PEI bear a positive charge. [25] To find the charge of the complex, the N/P ratio is therefore divided by 3. It is assumed that the ratio of RNA molecules to PEI molecules within each complex is the same as the overall ratio in the mix.

a) b)
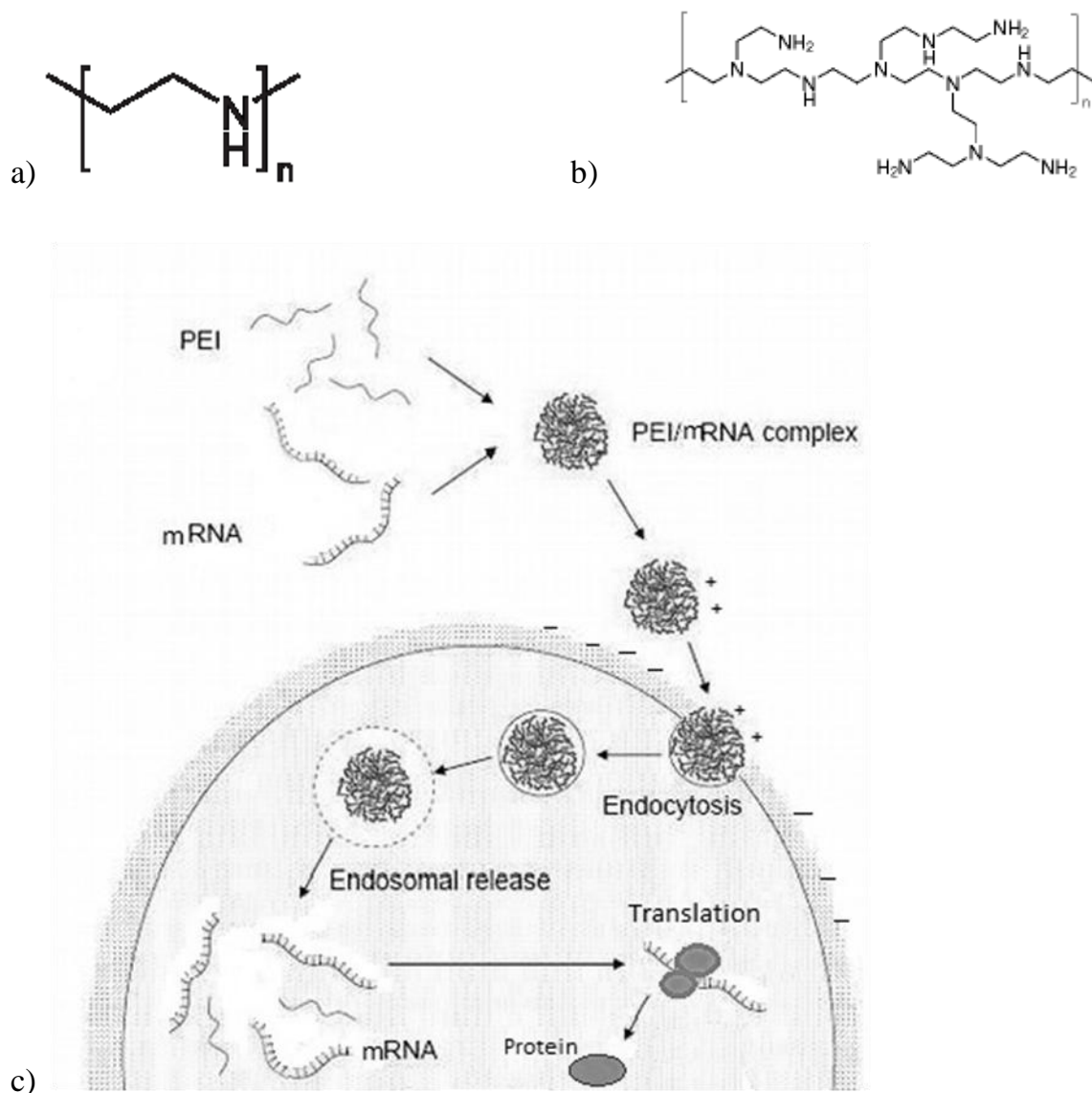
c)

Figure 1.2. (a) Monomer structure of PEI. (b) Branched PEI. [26] (c) Graphical summary of polyplex formation and internalization of mRNA molecules complexed with PEI. The polyplexes have a net positive charge, and adhere to the negatively charged plasma membrane by electrostatic interactions. Note that polyplexes consist of multiple RNA and PEI molecules. Figure adapted from Agner, [27].

The carrier shields the mRNA, protecting it from degradation by RNAses. The mRNA/carrier complexes have a net positive charge due to the higher concentration of PEI than mRNA in the mix, and therefore associate to the cell membranes, which have a net negative charge due to glycosylations and phosphorylations on surface proteins. [28] When the membrane with mRNA/PEI polyplexes attached is endocytosed, the polyplexes will be incorporated in the endosome as illustrated in figure 1.2c.

At high concentrations ($1.5*10^{-2}$ μg/μl), PEI itself causes rupture of endosomal membranes, presumably due to osmotic pressure caused by increased protonation level of PEI in the low pH conditions in the endosomes (the proton sponge effect), with subsequent influx of Cl^- and H_2O. [25] At low concentrations (below 10^{-2} μg/μl), the proton sponge effect is not strong enough to disrupt the endosomal membrane and PEI is thereby entrapped in the lysosomal pathway unless released by other agents.

β-cyclodextrin

A bio-compatible carrier was also assessed for use in mRNA transfection. Cyclodextrins (CDs) are a group of cyclic oligosaccharides forming a toroidal shape with a somewhat hydrophobic inside and a more hydrophilic outside caused by outwards oriented hydroxyl groups. [29] CDs are capable of forming inclusion complexes with hydrophobic particles of the right diameter. [30] CDs with six, seven or eight glucose units (α-, β-, and γ-CDs, respectively) occur naturally in the human body where they act in the transport of specific hydrophobic molecules. [31] CDs are widely used in biomedicine as solubilizers, stabilizers or excipients alone or covalently bound to other functional groups. [32] The CDs are generally considered as bio-tolerable, although some formulations, including β-CD, are nephrotoxic. [33]

β-cyclodextrin (1135 Da) consists of seven glucose molecules, giving a cavity diameter of 6.0-6.5 Å. [32] β-CD-based carriers have been characterized for use with oligonucleotides (siRNA), [34] but are not well described for mRNA transfection. A β-CD polymer linked with 6 methylene units (β-6CDP; figure 1.3), with M_w averaging 8.8 kDa corresponding to 6 units of β-6CD, and charge averaging +12 per

molecule, was used in this study. In contrast to monomeric β-CD, this polymer has good solubility. It is able to form complexes with nucleic acids based on electrostatic interactions. The resulting complexes are positively charged, and may therefore adhere to the cell surface by the same principle as PEI-based complexes. [35]
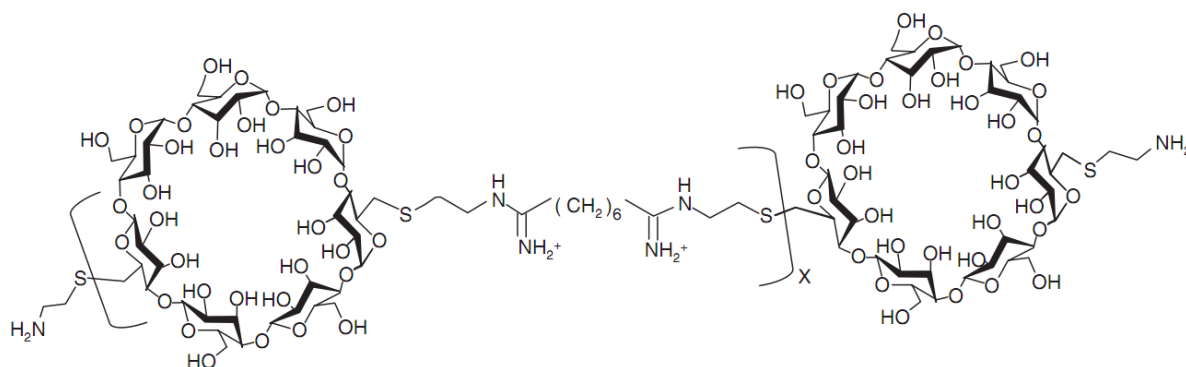
Figure 1.3: Structure of β-cyclodextrin polymer with 6 methylene units (β-6CDP). Figure from Bøe, [34].

Light directed gene delivery: PCI

The PhotoChemical Internalization (PCI) method was developed at the Radium Hospital for enhanced delivery of genetic material or other compounds into the cytosol of cells in a site-specific manner. [36] The method enables endocytosed material to escape the endocytic pathway by light-induced rupture of endosomal and lysosomal membranes.

An amphiphilic photosensitizing compound that is designed to be activated by light of a certain wavelength is added to the cells along with the drug to be delivered. The photosensitizing compound associates to lipids in the cell membranes. As the drug is endocytosed, photosensitizer molecules will be associated to the membranes of endocytosed vesicles.

When illuminated at the appropriate wavelength, the compound absorbs the light energy in its conjugated chemical bonds, producing highly reactive oxygen species (ROS), mainly singlet oxygen. ROS may induce damage to nearby molecules such as

fatty acids and thereby create holes in endosomal and lysosomal membranes leading to release of entrapped material into the cytosol. ROS have a very short reaction range due to antioxidative compounds in the cell. [37]

In clinical trials, PCI treatment has shown to mediate efficient drug delivery to cancer patients. [38] By illuminating the tumor only, the construct was taken up specifically by cells in the tumor, and the impact on the rest of the body was reduced. [39] In the current study, PCI treatment was assessed for use with the aforementioned system as a move toward *in vivo* applications.

1.3 Endocytosis

Endocytosis is a collective term for a range of mechanisms through which cells take up extracellular material. The endocytic pathways (summarized in figure 1.4) can be roughly divided into two groups;

- pinocytosis, which can be clathrin-dependent (~100 nm), caveolar (~50 nm), clathrin-independent or macropinocytosis (0.5-5 μm)
- phagocytosis, which happens primarily in cells of the immune system [40]
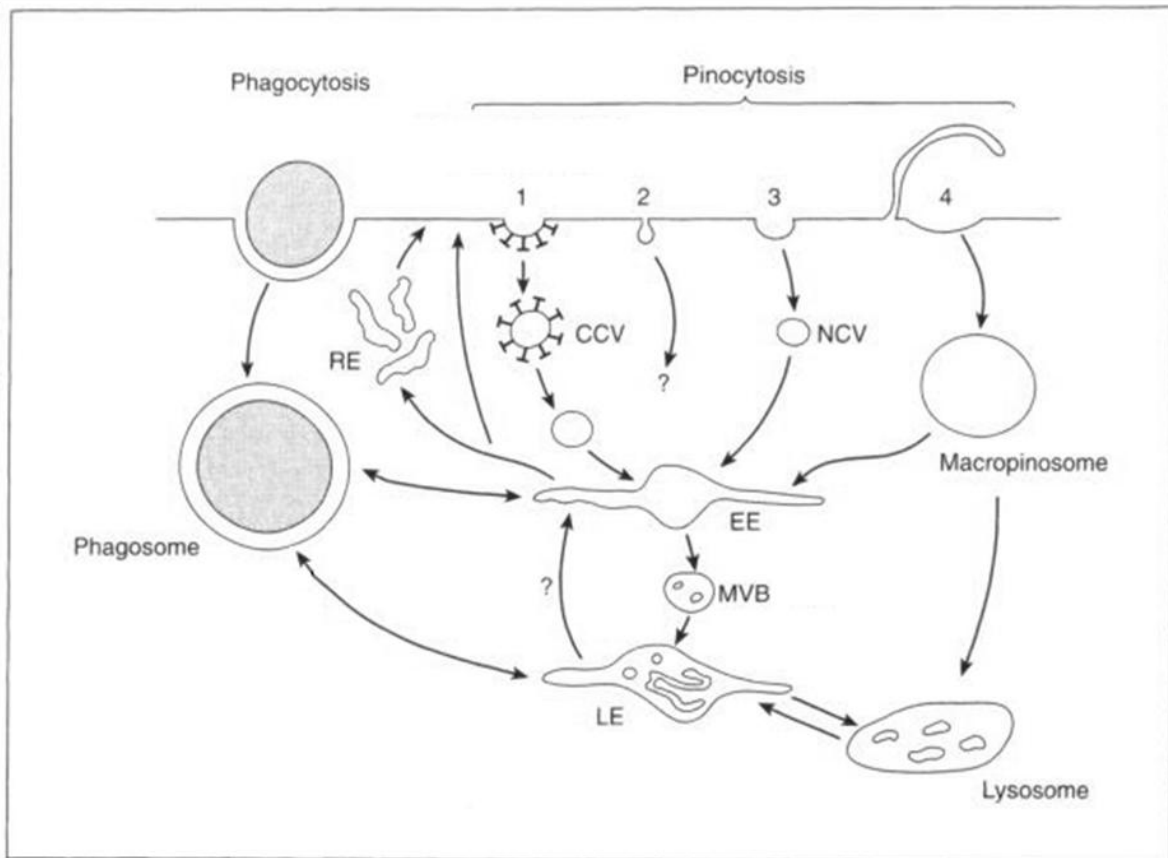
Figure 1.4: Summary of the endocytic pathways. Pinocytosis mechanisms pictured: 1. clathrin coated vesicles, 2. caveolae, 3. non-coated vesicles and 4. macropinocytosis. Figure from Marsh, [40].

Many of the steps involved remain obscure, and new mechanisms for endocytosis are still being discovered [41]. All pathways involve entrapping the material to be endocytosed in a pocket in the plasma membrane formed by cytoskeleton remodeling. The pocket is pinched off as a membrane-enclosed compartment in the cytosol, and typically fuse with an early endosome (pH 6). The pathway continues through endosomal compartments with a progressively acidic environment due to vascular H^+ ATPase activity, until arriving in the lysosome (pH 4.5-5). Acid hydrolases and other degrading enzymes in the endosomes and lysosomes are activated by low pH. [42, 43] Endocytic vesicles are very dynamic, often undergoing fusion and fission events.

Throughout the pathway, the cargo is trapped within membrane enclosed compartments and will normally not be in contact with the cytosol before it is digested in the lysosome.

Phagocytosis is the main internalization mechanism for particles exceeding 200 nm in size, according to Marsh. [40] Most phagocytosis occurs by the professional phagocytic cells of the immune system, but also other cell types, including fibroblasts and epithelial cells, are capable of phagocytosis. [44] Phagocytosis is initiated by cytoskeleton induced protrusions of the cell membrane around the particle, engulfing the particle in a large vesicle called a phagosome. Phagosome maturation parallels endosomal maturation, as illustrated in figure 1.5, also in terms of pH change, due to considerable exchange of material by vesicular transport or organelle fusion.
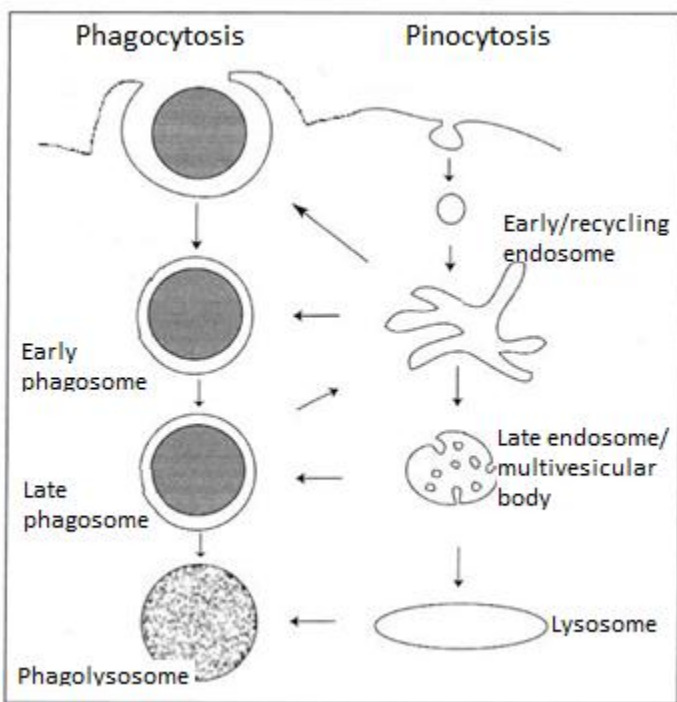
Figure 1.5: Phagosomal and endosomal maturation. From Rosales, [44].

Different cell types may have varying endocytic capacities by the different mechanisms. Inhibition studies of the endocytosis of particles of similar size to the particles used in the current study, suggest that multiple endocytic pathways contribute to the uptake. [45]

1.4 S100A4

S100A4, also known as Mts1, p9Ka or metastatin, is a human gene normally expressed in certain cell types including some types of immune and endothelial cells. The name refers to the solubility of the first identified S100 proteins in 100% saturated ammonium sulphate. [46] The gene codes for a small (101 amino acids per chain), usually di- or oligomeric protein with two Ca^{2+}-binding EF hands on each chain. [47] Upon Ca^{2+} binding the conformation of the protein is altered, exposing a hydrophobic pocket which can interact with target proteins. It thereby acts as a Ca^{2+}-sensor. [48] In the dimeric form, both S100 subunits form hydrophobic pockets and can thus bind two target proteins at the same time, bringing them together.

The reported cellular locations of S100A4 span from the extracellular space and cytosol to the nucleus. While the protein has no enzymatic activity on its own, it binds other proteins and influences their activity by altering their conformation. In the nucleus, it is presumed to modulate transcription of target genes. When secreted, it is reported to initiate auto- or paracrine signaling pathways. [49]

Ectopic expression of S100A4 in cancer affects several of the cancer hallmarks: angiogenesis, survival and metastasis, [49, 50] and is correlated with adverse prognosis for the patient (higher-grade tumors and shorter life expectancy). [51] S100A4 has been proposed as a prognostic marker in several cancers including colorectal cancer. [52] The gene tends to show up in expression profiles of cancerous cells from many cell type origins. This may be caused by the general hypomethylation often found in cancer. [53] Because of this, the gene has been subjected to a lot of interest from cancer researchers for years; however, its precise roles in cancer propagation are not yet fully elucidated at a molecular level.

Identifying target genes for the activator function of S100A4 is one approach to investigating the role of the protein in cancer propagation.

1.5 Aims of the study

The aim of the current study was to optimize a method for mRNA delivery into human cancer cell lines. Furthermore, to demonstrate that the strategy can be combined with microarray profiling to disclose interaction networks and reveal gene functions.

The S100A4 gene was chosen due to its ability to affect several of the hallmarks of cancer: angiogenesis, survival and metastasis. S100A4 has been characterized extensively by others, often by removing the expression of the gene using e.g. siRNA molecules. [52, 54, 55] In order to validate these findings by another approach and possibly identifying novel target genes, a method for transfecting cells with mRNA was optimized for two human cancer cell lines (OHS and LOX). Two different carriers were tested for mRNA transfection. In addition, we explored the possibility for targeted mRNA delivery by combining with PCI, a promising strategy for site-specific transfection *in vivo*.

2. Materials and Methods

2.1 Cell work

The aims of the study involved optimizing a method for mRNA delivery into cells, and demonstrating the possibility to disclose novel S100A4 gene interactions after expression profiling. For these applications human cancer lines are preferable to work with, as cultured cells are easy to grow and transfect in a controllable manner.

2.1.1 Cell culture

Two different human cancer cell lines with well characterizes S100A4 status were used in the study; the osteosarcoma cell line OHS which has high S100A4 expression, and the melanoma cell line LOX, which is negative for S100A4 expression. Both cell lines were established from patients at the The Norwegian Radium Hospital, and have been cultivated for several years. [56, 57]

Cells were grown in 75 cm^2 flasks (Nunc, Roskilde, Denmark) containing RPMI medium (BioWhittaker, Verviers, Belgium) with 2mM L-glutamine (GlutaMAX; GibcoBRL, Paisley, UK) and 10% fetal calf serum (FCS; BioWhittaker, Verviers, Belgium) at 37°C in humidified atmosphere containing 5% CO_2. Cell cultures were passaged two to three times per week by adding 1 ml trypsin (BioWhittaker) when reaching approximately 90% confluency. Trypsin is a serine protease that breaks down the extracellular proteins that adhere cells to the surface of the vessel. 1/8 to 1/10 of the cell culture was passed on in each passage. The remaining culture was used for seeding or discarded.

2.1.2 Plating of cells

In order to seed the correct number of cells, suspended cells were counted using a manual click counter and a Bürke chamber (Kova Glasstic; Hycor, CA, USA); a microscope slide with a chamber accommodating a fixed volume of cell culture and a grid for counting.

For the OHS cell line, approximately 80 000 cells were plated per well in 6-well plates or approx. 45 000 in 12-well plates. The LOX cell line divides slightly faster, and approx. 75 000 and 41 000 cells were plated, respectively. Cells were incubated at 37°C for approx. 48 hrs until cells were 50-60% confluent.

2.1.3 Freezing and thawing cells

In a cell culture that is allowed to run for an extended period of time, random mutations will accumulate in the genomes of the cells, possibly altering the properties of the cell culture over time. In order to minimize such variation, cell cultures were not allowed to run for more than ~2 months before being replaced by a fresh cell culture batch.

Below -150°C is defined as cryogenic temperature. [58] At cryogenic temperature, cells are virtually indefinitely stable. [59]

Freezing procedure:
When needed, cells were frozen by a slow-freeze method using dimethyl sulfoxide (DMSO; Sigma-Aldrich) as a cryoprotectant, preventing formation of damaging crystals in the freeze-culture.

DMSO is toxic to metabolically active cells and should therefore be added immediately before freezing. Rubber gloves should be used as the compound dissolves nitrile.

Prior to freezing, medium was discarded from a 90-95% confluent, actively growing cell culture. Cells were detached from the surface by the use of 1 ml trypsin. After detachment, cells were diluted in 10 ml medium, and 9 ml of the suspended cell

culture was pelleted and re-diluted in 9 ml freeze medium (Appendix E). The rest of the cell culture (1 ml) was passaged, except for 100 μl, which was used for testing against Mycoplasma infection. The freeze medium was divided into 9 labelled microvials and slow-frozen for 24 hrs at -80°C in a Nalgene Cryo freezing container (Thermo Sci) filled with isopropanol. The freezing container was then transferred to a -180°C freezer. After 24 hrs at -180°C the microvials were transferred from the freezing container to a separate "quarantine" box. The microvials were kept in the quarantine box until the Mycoplasma test was confirmed negative.

Thawing procedure:

The cell vial was transferred directly from -180°C to 37°C for rapid thawing. The vial was desinfected with 70% EtOH before opening. Once liquid, the cell culture was immediately transferred to a 75 cm^2 cell culture flask and an ample amount of growth medium was added to dilute the freeze medium. When the cells adhered to the bottom surface (after 24-30 hrs), the medium was replaced with fresh medium to remove residual DMSO.

The morphology and gene expression profile of newly thawed cells may differ from normal. The culture was therefore passaged at least two times before use in experiments.

2.1.4 Mycoplasma testing

All cell lines were routinely tested for Mycoplasma infection using the PCR (Polymerase Chain Reaction)-based VenorGeM® Mycoplasma Detection kit (Minerva Biolabs, Berlin, Germany) by in house laboratory staff every 6 weeks. At 90-95% cell confluence, 100 μl of medium was transferred from culture flasks to sterile microtubes and stored at -20°C until analyzed. PCR was performed using primers specific for the conserved 16S rRNA coding region in the Mycoplasma genome, allowing for detection of *Mycoplasma*, *Acholeplasma*, and *Ureaplasma* species. [60]

2.2 Transfection

Transfection is a method for transferring macromolecules, usually genetic material, into cells. In this study, messenger RNA (mRNA) for our gene of interest was transfected into two different human cancer cell lines and used by the cells as a transient template for producing protein.

Multiple transfection protocols are available for mRNA transfection, including microinjection, electroporation, and complexation with lipid or cationic excipients. The transfection carrier serves two purposes:

- Transporting the mRNA through the cell membrane.
- Protecting the easily degradable mRNA molecules until arrival in the cytosol, where the mRNA must become accessible for the translation machinery.

All transfection implies transport through the cell membrane, compromising the barrier that ensures homeostasis within the cell. Extensive optimizations were performed in order to minimize cell toxicity while obtaining high transfection efficiency.

Transfection procedure

Both cell lines were transfected transiently with S100A4 mRNA at 50-60% confluency (~0.5 – 1 x 10^6 cells) two to three days after seeding, using 25 kDa branched PEI (Sigma-Aldrich) or 8.8 kDa β-6CDP (Gift from Mark E Davis, California Inst. of Technology) with or without PCI technology (described below).

Transfection agent and mRNA were added to 200 µl serum-free medium and allowed to form complexes for 30 minutes. After complex formation, the complex solution (200 µl per transfection) was added to wells containing cells and 800 µl serum-containing medium.

For PEI-based transfections, a broad concentration assay was used initially, before converging on the concentrations that showed the highest transfection efficacy with

lowest cytotoxicity. For β-6CDP-based transfections, three concentrations that had shown good efficiencies in earlier siRNA based studies [34] were selected for use with mRNA. Typical amounts of transfection reagent and mRNA are listed in table 2.1.

Table 2.1: a) Typical ratios of mRNA and PEI used in non-PCI (top) and PCI-assisted (bottom) transfections. b) Amounts of β-6CDP and mRNA used in β-6CDP-based transfections. All amounts are given as µg per tranfection. All complexation was done in 200 µl serum-free medium.

PCI	PEI (µg)	RNA (µg)	N/P
-	3.0	1.0	22
-	3.0	2.0	11
-	3.0	3.0	7.3
+	0.4	1.0	3
+	0.7	1.0	5
+	1.1	1.0	8
+	1.4	1.0	10

a)

PCI	β-6CDP (µg)	RNA (µg)
+	12.5	1.0
+	25	1.0
+	50	1.0

b)

2.2.1 Transfection using PCI

The PhotoChemical Internalization (PCI) method (introduced in section 1.2.1) was used in some of the experiments to investigate the possibility for enhanced transfection efficiency in a site-specific manner. The photosensitizer used in the light-enhanced experiments was meso-tetraphenylporphine with 2 sulfonate groups on adjacent phenyl rings (TPPS$_{2a}$; Frontier Sci, Logan, USA. See figure 2.1).
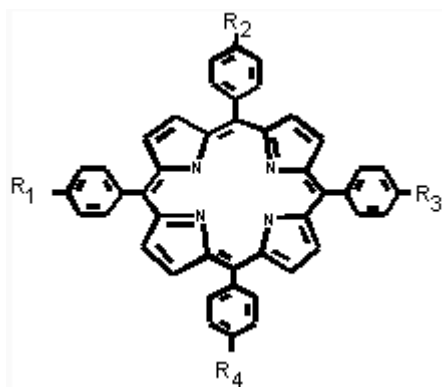
Figure 2.1: TPPS structure. In TPPS$_{2a}$, 2 neighboring R groups are sulfonate. The molecule is extensively conjugated, absorbing light at 420 nm.

This amphiphilic photosensitizer localizes to the cell membranes, and will be internalized in endocytic vesicles. When treated with blue light, an oxidative reaction is initiated which leads to membrane damage and subsequent release of endocytosed material including mRNA/carrier complexes into the cytosol where mRNA is translated.

Procedure:

mRNA/PEI complexes were prepared as described in section 2.2.1. For PCI treatment, 8 µl TPPS$_{2a}$ was added to 12.5 ml RPMI medium containing serum and glutamine. 800 µl of the sensitizer-containing medium was added to each well, along with 200 µl of mRNA/PEI complexes, giving a final TPPS$_{2a}$ concentration of 0.5 µg/ml. After an 18 hours incubation, cells were washed three times to remove excess photosensitizer followed by a 4 hrs re-incubation step (chase) prior to 30 seconds of illumination (peak wavelength 420 nm) using a LumiSource light source (7 mW/cm^2; prototype, PCI Biotech, Oslo, Norway). The washing steps with the following chase reduces cell membrane damage as a large portion of the photosensitizer in the cell membrane will be either washed away or renewed during the 4 hrs incubation time. Expression analyses were performed after 20-24 hours. All procedures involving TPPS$_{2a}$ were conducted in dimmed light, and cells treated with TPPS$_{2a}$ were protected from light using aluminum foil.

2.2.2 Particle size measurement

Particle size can be operationally defined as the diameter of a sphere that diffuses at the same speed as the particle being measured.

Particle size is calculated from the Brownian motion, the "random walk" observed in all particles in solution. The speed of the random motion is proportional to particle size. [61] Information about the size and dispersity of transfection particles can give clues about the mechanisms that can act in their internalization.

Procedure:

Particle sizes of transfection polyplexes were measured using a Zetasizer Nano-ZS (Malvern Instruments, Worcestershire, UK) with software Zetasizer 6.01 using a pre-defined protocol (SOP) that contains information about the solvent, the cuvette used in the measurements, and expected range of particle sizes.

Polyplexes were prepared as described in section 2.2.1, and allowed to assemble for 30 minutes. 60 µl of the complexation mix was used to measure particle sizes in a micro cuvette (ZEN0040; Malvern). The measured particle sizes were exported to a text file.

Incubation time is an important factor influencing complex size, and each measurement takes a significant amount of time (3 minutes). The position of each sample in the measurement series is therefore expected to influence the measured particle size. To minimize this effect, the sample order was randomized.

2.3 Flow Cytometry

Flow cytometry is a very accurate, efficient, and reliable method for the detection of light scattering, as well as fluorescence in individual cells. Cells travel past the lasers one cell at a time in a fluid stream (figure 2.2). Scattered light is detected and information about size, granularity and fluorescence for the individual cells is derived

from the scattering pattern. Forward scatter (FSC) is detected at angles close, but not equal to the direction of the laser beam. Reflection at small angles gives information about cell size. Side scatter (SSC) is detected at angles close to 90°. Reflection at wide angles gives information about the granularity (amount of solid content) within the cell. [62]
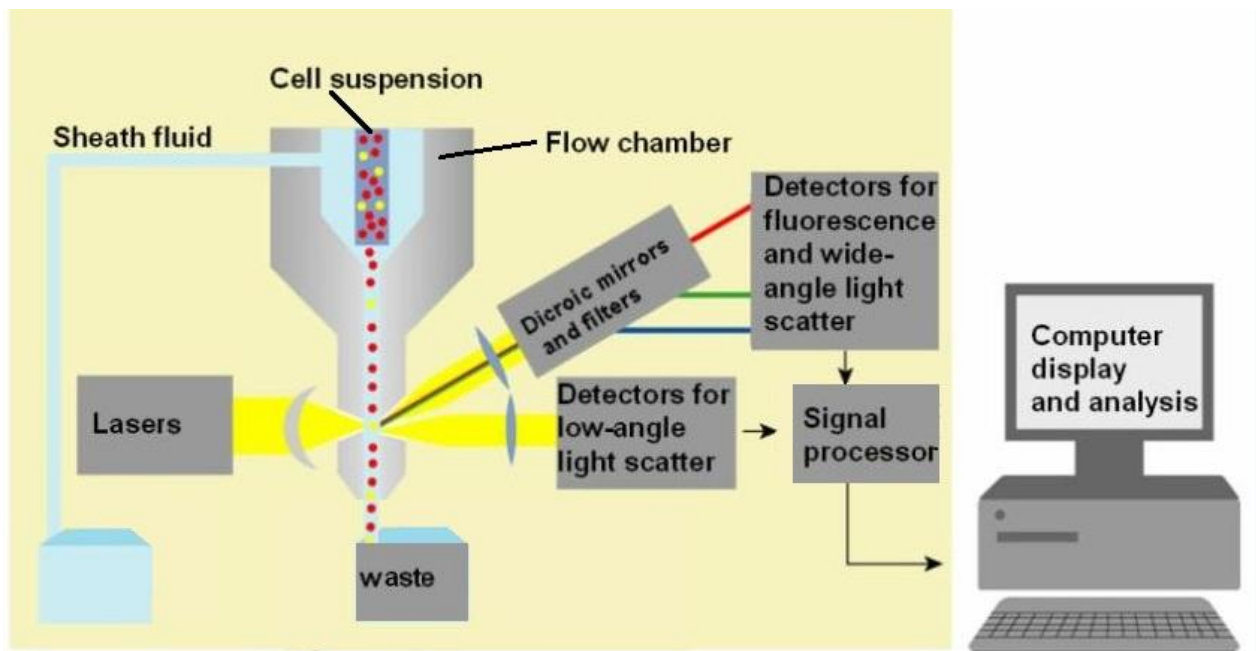
Figure 2.2: Flow cytometer diagram. Adapted from Strand, [63].

In the present study, a BD LSR II flow cytometer (BD Biosciences, NJ, USA) was used to quantify expression of a transfected protein, in order to assess transfection efficiency. As S100A4 cannot be detected by flow cytometry, the fluorescent reporter protein EGFP (enhanced green fluorescent protein) was used as a substitute. Transfection efficiencies using EGFP and S100A4 mRNA are assumed to be comparable in this experiment. EGFP has its absorption maximum at 489 nm and emission maximum at 509 nm (see figure 2.3).

The nucleic acid intercalating agent propidium iodide (PI; Invitrogen, Carlsbad, USA) was used to detect dead cells. This fluorochrome enters through holes in the membranes of dead cells, and is generally excluded from live cells when using low concentration and short incubation time. When bound to DNA or RNA, it emits a red light with peak at 620 nm when excited at 561 nm. ([64], page 46)

Procedure

Cells were transfected according to section 1.2.1 with or without PCI treatment. 24 hrs after transfection, cells were trypsinized, resuspended in 750 µl growth medium and transferred to flow cytometry tubes with a cell-strainer filter cap (Falcon; BD Biosciences). The filter cap removes cell aggregates. 1 µl PI was added to each sample just prior to analysis.

EGFP and PI were excited at 488 and 561 nm, respectively. Emitted light at 510-520 and 622-630 nm was detected (see figure 2.3). 10 000 events were recorded per sample. Events include not only cells but also cell fragments and other particles that may be present in the suspension.

Results obtained were analyzed on FACSDiVa software version 6.1.2. PI positive cells, cell fragments, and doublets not removed in the filtration step (particles of large size, determined from a large side scatter) were excluded from the analysis as seen in figure 2.4.

a)

b)
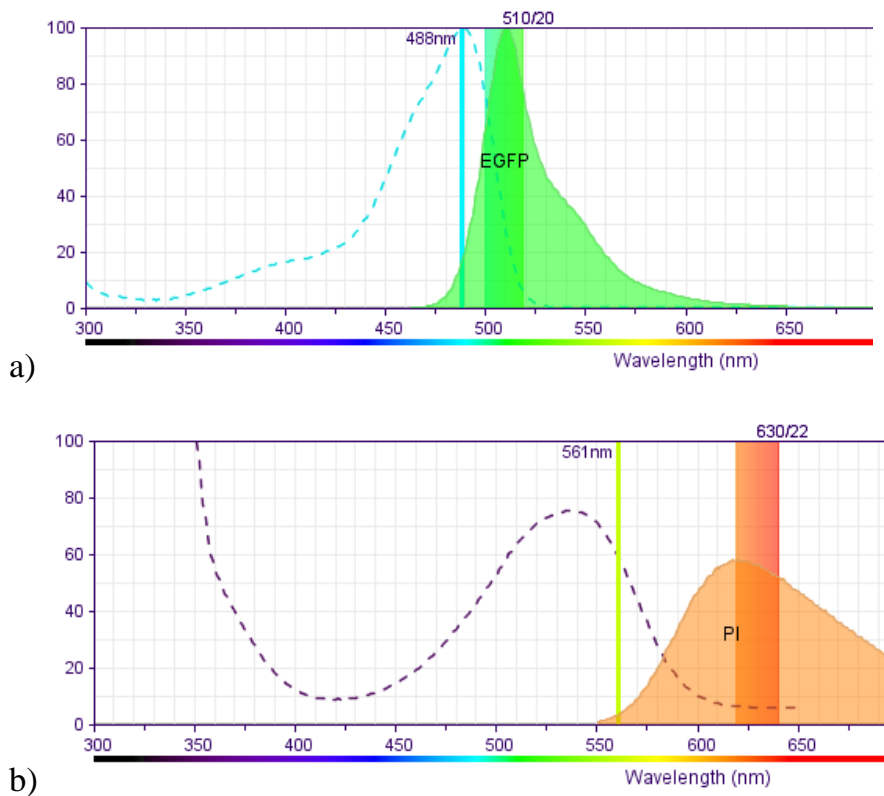
Figure 2.3 shows EGFP (a) and PI (b) spectra plotted with wavelength on the horizontal axis and relative brightness on the vertical axis. Excitation spectra are shown with dotted lines, emission spectra in solid color. The laser used for excitation is shown with a vertical line. The figure was made by using BD software [65].
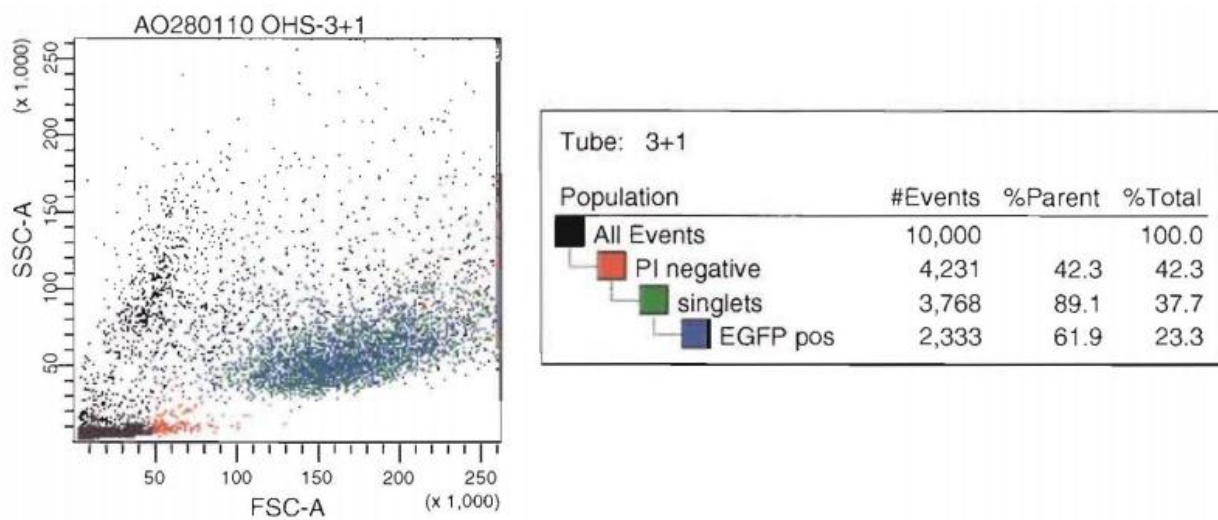
Figure 2.4: Screen shot of FACSDiVa flow cytometer software. In this example, EGFP transfection efficiency is 61.9% in living single cells. EGFP positive, single, PI negative cells are shown as blue spots in the scatter plot to the left.

2.4 Microscopy

EGFP transfected, fluorescent cells were also viewed in a fluorescence microscope with a 488 nm filter (Axiovert 200M, Zeiss, Obercochen, Germany) for an overview of the transfection efficiency as well as cell confluency and morphology within each sample. Images were captured using the associated AxioCam CCD camera and processed using AxioVision software.

2.5 RNA expression analyses

Two different strategies for quantifying mRNA were employed in the study.

qPCR is a very sensitive method for quantifying the expression of a smaller number of genes of interest. A typical workflow would be as follows; isolating RNA from harvested samples, transcribing the RNA to the more stable form DNA (denoted *cDNA* where c stands for copy), designing specific primers for the gene(s) of interest following detection of expression levels by qPCR.

When quantifying the expression of a large number of genes, qPCR quickly becomes very laborious and time-consuming. An expression microarray experiment profiles the entire transcriptome in one run, measuring the level of transcription of each gene in the genome of the relevant species. An expression profile gives very comprehensive information, but at a relatively high cost.

2.5.1 Isolation of RNA

20 hours following transfection, total RNA was isolated using GenElute Mammalian total RNA Miniprep kit (Sigma-Aldrich) as described in the manufactures protocol with the following adaptions:

- Cells were lysed directly in the wells using freshly prepared lysis solution/2-mercaptoethanol mixture.
- In the final eluation, the eluation solution was transferred back on the column for a second eluation in order to increase yield.

RNA concentration and A_{260}/A_{280} ratio were measured using a Picodrop spectrophotometer (Thermo Fisher Sci, Waltham, USA). RNA and DNA absorb light at 260 nm, whereas protein (aromatic residues) absorbs light at 280 nm. An absorbance ratio of 260/280 nm below 1.8 implies protein contamination in the sample. All samples were stored at $-80^{\circ}C$.

2.5.2 Precipitating RNA

When necessary, RNA samples were precipitated to increase concentration using the following protocol:

- Add 1x volume isopropanol and 0.1x volume sodium azide
- Precipitate over night at $-20^{\circ}C$
- Centrifuge for 40 minutes at maximum speed (13 000x G or more) at $4^{\circ}C$.
- Carefully remove the supernatant.
- Wash the pellet with ~100 µl 75% EtOH
- Centrifuge at maximum speed, 15 minutes
- Remove supernatant, dry the pellet for a few minutes with open lid. Too long air dry will impair solubility.
- Dissolve the pellet in the desired volume of the eluation buffer used in RNA isolation.

2.5.3 DNAse treatment

When necessary, traces of DNA were removed using DNAse. This was done prior to amplification of transcripts lacking introns. For treatment of 1 µg RNA; 1 µl DNAse I, 1 µl buffer and RNAse free H_2O to a total volume of 20 µl (all reagents: Invitrogen) were added. Samples were incubated at room temperature for 15 minutes; DNAse was then inactivated by adding 2 µl EDTA and incubating samples for 10 minutes at $65^{\circ}C$. Samples were kept on ice and centrifuged briefly prior to further analyses.

2.5.4 cDNA synthesis (reverse transcriptase PCR)

cDNA was prepared from 1 µg of total RNA in PCR tubes (200 µl) using qScript cDNA synthesis kit (Quanta, Gaithersburg, USA) containing random and oligo-dT primers, enabling reverse transcription of total RNA content.

The reaction was done on a GeneAmp PCR System 9700 thermal cycler (Applied Biosystems, Foster City, USA) programmed using table 2.2.

Table 2.2: Temperature cycle used in cDNA synthesis.

Temperature	Time	Function
25 ^{o}C	5 min	Stabilizing samples
42 ^{o}C	30 min	Annealing primers, transcription
85 ^{o}C	5 min	Denaturing
4 ^{o}C	Storage	

cDNA was stored at 4°C. Assuming 100% reaction effectiveness, the cDNA concentration is 50 ng/µl. Prior to quantitative PCR, all samples were diluted with sterile H$_2$O to 15 ng/µl.

2.5.5 Quantitative PCR

Quantitative PCR (qPCR) was used to compare the amounts of mRNAs of interest between samples. The iQ SYBR Green Supermix (Bio-Rad, Hercules, USA), containing dNTPs, iTaq DNA polymerase, dsDNA-activated fluorescent dye and buffer, was used for the reactions. Primers (forward and reverse strand) for the gene in question were used along with primers for two household genes; RPLP0 (large ribosomal protein) and TBP (TATA binding protein).

Primer design

Custom primers were designed using the Roche Universal probe library [66] and PrimerBlast [67] online tools and quality controlled using the following criteria (in accordance with [68]):

- Transcript length 60-90 bases
- Primer length 18-21 bases
- GC nucleotide content 50-65%
- Melting temperature (T_m) preferably 58-61°C
- Dinucleotide repeats of more than 3 repeats and single base repetitions of more than 3 bases were avoided
- Primer candidates were analyzed for secondary structures (hairpins and dimerizations) using the IDT OligoAnalyzer [69].

All primers were purchased from MedProbe (Oslo, Norway) and diluted to 10 pm/µl before use. Primer sequences are listed in Appendix C.

qPCR procedure

Master mixes containing iQ Supermix, primers, and sterile H_2O were prepared according to the manufacturer's direction (see Appendix E), one master mix per pair of primers.

Master mixes were distributed carefully into PCR tubes (one tube per sample), 50 µl per tube. 10 µl of cDNA template was added to each tube. A negative control containing H_2O in place of cDNA was prepared for each of the master mixes. Each sample was distributed in two wells in a 96-well PCR plate (25 µl per well) and the plate was sealed with optical film (Bio-Rad).

The qPCR reaction was run on an iCycler thermal cycler (Bio-Rad) with iCycler software version 3.1.7050 programmed with the following temperature cycle (listed in table 2.3): Initial denaturation to separate compatible cDNA strands and activate the engineered polymerase, followed by 42 cycles of annealing and denaturing (steps 2 and 3). In the final cycle, the denaturing step was extended to ensure full strand separation, after which the samples were gradually cooled down.

Table 2.3: qPCR temperature cycle. Steps 2 and 3 are cycled 42 times before going to steps 4 and 5.

Step no.	Temperature	Time	Function
1	95 $^{\circ}$C	3 min	Initial denaturation
2	60 $^{\circ}$C	35 sec	Annealing
3	95 $^{\circ}$C	10 sec	Denaturation
4	60 $^{\circ}$C	35 sec	Annealing
5	95 $^{\circ}$C	20 sec	Denaturation
6	6 $^{\circ}$C		Storage

Data analysis

Intensity curves were viewed in iCycler iQ software version 3.1 (figure 2.5), removing any curves with dropping intensities from further analysis. Threshold position (the intensity corresponding to the threshold cycle C_t) is set at the beginning of the linear area of the curves, separated from the baseline level.
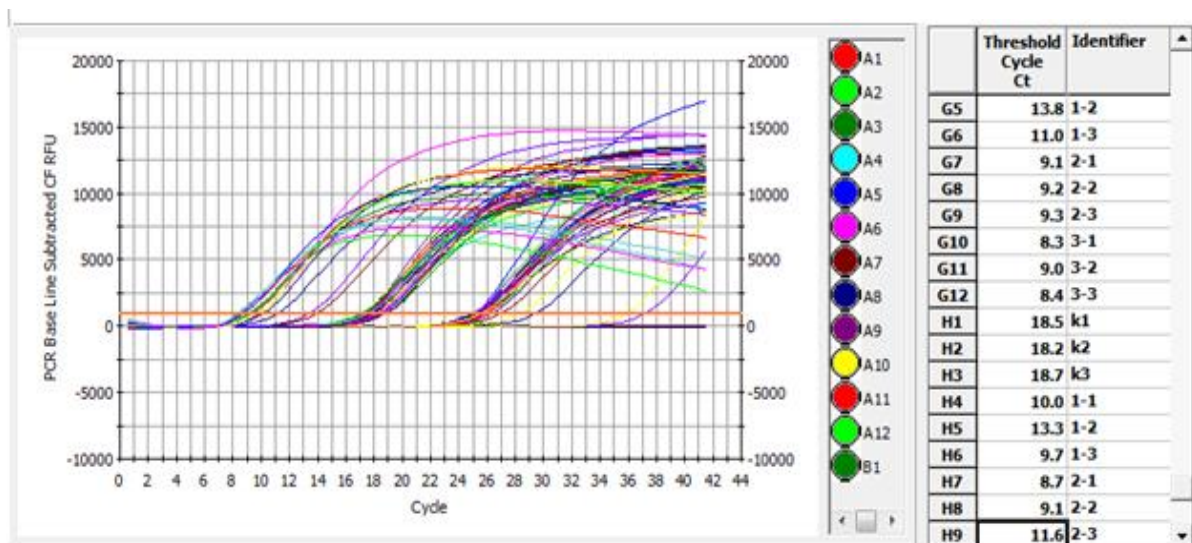

Figure 2.5: Intensity curves from a qPCR experiment as viewed in iCycler. Baseline fluorescence (the fluorescence detected in the initial cycles) is set as 0. Threshold position is labeled in orange. Genes are rising above threshold level at different time points, forming separate groups.

2.5.6 polyacrylamide electrophoresis of DNA

Whenever a new protocol or new primers were employed, the sizes of the PCR products were controlled by DNA electrophoresis. Acrylamide gels were prepared in a dedicated PCR lab, as described in appendix E, and poured into a 15-well electrophoresis cell (Bio-Rad). When solid, 7 µl of qPCR product and 1.5 µl of nucleic acid loading buffer (Bio-Rad) was added to each well along with a λ HindIII DNA ladder (BioRad). The electrophoresis was run at 180V for 20 minutes using TAE (buffer composed of Tris base, acetic acid and EDTA) as the running buffer.

The gel was then transferred to a container filled with TAE. 4 µl of nucleic acid gel stain (SYBR gold, Invitrogen) was added. The gel was transferred to another container of TAE to remove excess stain and photographed in a Gel Doc 2000 UV camera (Bio-Rad) using the associated software Quantitation One. The size of the amplified DNA molecules were compared with the known size of the transcripts created in the RT-PCR as a control for incorrect amplification products.

2.6 Microarray experiments

Part two of the project concerned downstream genes of our model gene, S100A4. By altering S100A4 expression with following expression profiling, we were aiming to identify genes that are influenced by S100A4 expression. This explorative approach is only possible when using profiling methods.

Microarray technology measures the transcription level of thousands of genes in parallel (simultaneously) from a single RNA sample. This makes it possible to obtain a snapshot of the transcriptome of the cells. The procedure is highly automated, ensuring replicability of the data.

Several platforms for microarray experiments are available, all utilizing the ability of nucleic acids to base pair to a specific nucleic acid probe. The base paired nucleic acids are detected, usually by fluorescence emitted by the probe.

The Illumina microarray platform utilizes beads covalently bound to specific probes and a detectable tag for each probe (see figure 2.6). Each individual bead is bound to several identical probes. There may be more than one probe corresponding to each gene. The beads are distributed randomly across silicon slides, and the positions of the tags are detected in each individual array. On average, each array contains 30 copies of each bead type.

One sample is applied to each array. Upon hybridization of samples to arrays, hybridized beads fluoresce. The fluorescence is captured as a high-resolution image, and the fluorescence intensities in each spot are analyzed. [70]
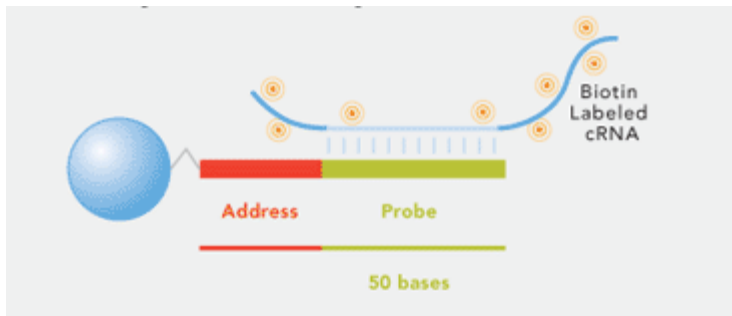
Figure 2.6: Bead with 23 bp code tag and a 50 bp probe, hybridized to biotinylated cRNA. The bead is 3 μm across, and bound to several probes (only one is shown).

The data sets produced in a microarray experiment are vast, and require powerful software for data analysis.

Experimental design

Cells were transfected with 3 μg S100A4 mRNA, a dose which had shown high transfection yield after qPCR quantification. To monitor the relationship between dose and response, cells transfected with a lower dose of mRNA (1 μg) were also included in the analysis. Cells transfected with EGFP mRNA were used as a negative control. EGFP is presumed not to interact with other genes as the EGFP gene is foreign to the human cell. Ideally, only unspecific effects of the transfection itself should affect transcription in these cells. The experiments were done in two different

cell lines (LOX and OHS) to assess reproducibility across cell lines. Two biological parallels were used for each parameter, giving a total of 12 samples, as listed in table 2.4.

Table 2.4: Type and amount of mRNA used in the two different cell lines tested. Two parallels were made for each parameter, giving a total of 12 samples. 3 µl PEI was used as the transfection agent in all transfections.

Gene	Amount	Cell line
S100A4	1 µg	OHS
S100A4	1 µg	LOX
S100A4	3 µg	OHS
S100A4	3 µg	LOX
EGFP	3 µg	OHS
EGFP	3 µg	LOX

Total RNA was submitted to the Norwegian Microarray Consortium (NMC) Microarray Core Facility at the Norwegian Radium Hospital.

The following procedures were done by in house laboratory staff at the facility:

Small samples of the submitted RNA were quality checked on the Bioanalyzer 2100 (Agilent, Santa Clara, USA). The Bioanalyzer separates the contents of the sample electrophoretically in microcapillaries. The distribution of RNA lengths is compared to a known distribution from the cell type in question. A shift towards shorter lengths indicates degradation of the sample. [71] The level of degradation is determined mainly from the ratio of the 28S to 18S rRNA peaks, which approach 2:1 in undegraded samples,[70] and is summarized in the RNA integrity number (RIN). RIN ranges from 1-10 where 10 indicates a very intact sample. RIN for samples used in microarray experiments should be above 7. [72]

The RNA must be amplified in order to obtain a detectable signal in the microarray. As there are no known enzymes that make RNA from an RNA template, it must be transcribed to DNA first. Reverse transcription was done using oligothymine primers to generate cDNA from mRNA only. The primers include an upstream T7 promoter

region for use in the subsequent cRNA synthesis. After first strand synthesis, the RNA template was degraded and the second strand cDNA was transcribed.
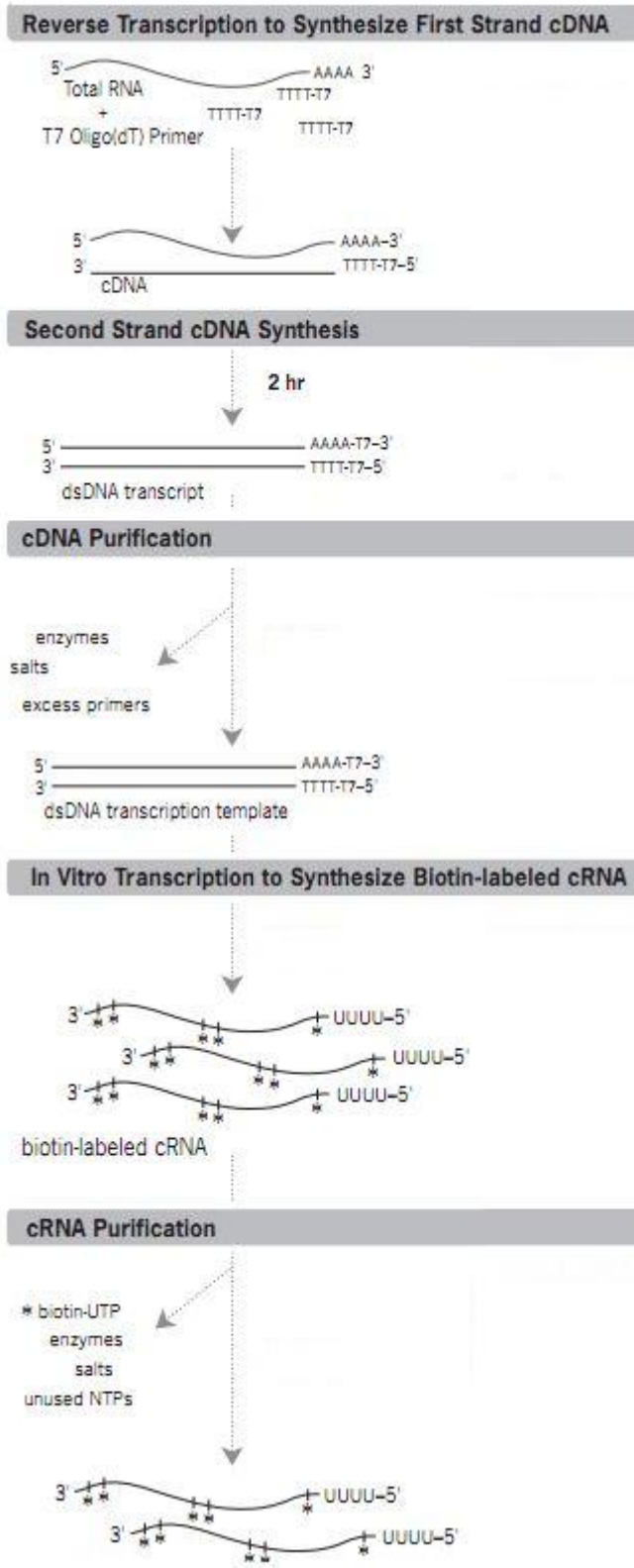
The double stranded cDNA was purified, and amplified as cRNA by T7 RNA polymerase in several cycles using a mix of unlabeled and biotin-labeled nucleotides.

cRNA was quality controlled to assess integrity, purity, and concentration of the samples.

The amplification procedure is summarized in figure 2.7.

Figure 2.7: Preparation of samples for the microarray experiment. Straight lines denote DNA, curled lines denote RNA, and asterisks denote biotin. Figure adapted from [70].

The labeled cRNA was hybridized to a Sentrix BeadChip array with a HumanHT-12 v4 probe set containing 47 000 probes covering the human transcriptome. The probe sequences in this probe set are derived from the gene database RefSeq.

Unhybridized cRNA was then washed off the array and the amount of bound cRNA on each bead was detected using streptavidin-Cy3. The Cy3-labeled streptavidin binds strongly to the biotin in the cRNA. Cyanine 3 is a fluorescent marker that emits green light at a wavelength of ~570 nm when excited at ~550 nm. Scanning of the slides was performed on a BeadArray Reader. The read-out from the scan results in large image files in which each bead shows up as spots of different brightness. Bright spots correspond to actively expressed genes. The data is converted to text files using the associated BeadStudio software, normalized and returned to the user along with the image files, a quality report including cluster analysis, and protocol files.

2.6.1 Bioinformatic tools used in the analysis of microarray data

The dataset was analyzed using the analysis software J-express [73] developed at the University of Bergen to identify genes that were significantly differentially expressed between experimental groups, with the help of Vegard Nygaard. The replicates were grouped together in the analysis. Different probes within the same genes were not grouped together, as some transcript variants may not span all probes. Quantile normalization and filtering to remove non-influenced genes was applied before analysis.

The main analysis utilized for this study was the unparametric test statistic Rank Product, a robust test for few-replicate, normalized microarray datasets. [74, 75] The rank a gene is given takes into account both the difference in expression between the experimental groups, and the variation between parallel samples. Higher rank indicates higher probability of a real difference in expression. The analysis also gives a q-value for each gene. The q-value is a False Discovery Rate (FDR) adjusted p-value; one of multiple options for multiple testing adjustment of the p-value. If a list

of genes is cut off at q=0.05, 5% of the entries in the list are expected to be false. Settings used for Rank Product: 400 permutations, random seed. Additionally, the Fold change viewer was used to envision distributions and magnitudes of expression changes.

A set of six candidate genes was forwarded to qPCR validation based on the following criteria:

- High rank, corresponding to being significantly influenced by the treatment. Preferentially in both cell lines included in the experiment.
- Being relevant for one of the hallmarks of cancer, as determined by researching literature.

Overrepresentation analyses were carried out by using the web based tool DAVID [76, 77] developed at the National Cancer Institute, US. This was done by matching each gene to a set of Gene Ontology terms, and then comparing the occurrence of each term to its occurrence within a random list of genes from the same organism.

2.7 Protein analyses

The fact that a gene is detected on the mRNA level is often taken as proof of protein expression. There are, however, several points of regulation before an mRNA is translated to protein. Some mRNAs are translated at a low level, or not at all, due to properties of their sequence causing the RNA strand to be sequestered or degraded. Protein expression analyses are hence necessary to know that the gene is actually translated.

Unlike nucleic acids, protein is not easily amplified or sequenced. Immunological methods have thus proven invaluable for the indirect identification of protein. A typical workflow for the analysis of protein expression is to make lysates of the samples, measurement of the protein concentration before separating the proteins electrophoretically. The separated proteins are then transferred to a more durable

membrane material, and proteins of interest can be detected based on specific interactions with antibodies.

2.7.1 Protein lysate

Cell lysates for use in protein analyses were prepared using the following protocol:

- Medium was removed by pipetting
- 1 ml PBS was added to each well
- Cells were detached using a cell scraper
- Suspension was transferred to Eppendorf tubes and pelleted by centrifuging at 2000 RPM for 5 minutes
- Supernatant was removed by pipetting, and the pellet was frozen at -70 ^{o}C or -180 ^{o}C
- 25 µl lysis buffer (Appendix E) with protease inhibitors was added to frozen pellet
- Cells were lysed on ice for a minimum of 15 minutes with repetitive vortexing steps. Cell lysates were then sonicated at 4°C by dipping the probe in the lysate for 3x3 seconds
- Next, cell debris was pelleted by centrifuging at 15 000 RPM for 15 minutes at 4°C
- Finally, the supernatant was transferred to new tubes and stored at -70°C.

Of note, sonication causes the nuclear membrane to rupture, releasing nuclear proteins to the lysate.

2.7.2 Measuring protein concentration

The Bradford analysis of protein concentration utilizes a color reaction that can be quantified by spectrophotometry. The binding of the aromatic dye Coomassie Brilliant Blue G-250 (Bio-Rad) to protein changes the absorption maximum (A_{max}) of the solution from 465 nm to 595 nm. [78] By using a dilution curve of a reference protein with a known concentration, the concentration of the protein in the sample can be inferred.

The dye binds primarily to Arginine side chains, and slightly to other basic and aromatic residues. [79] The amino acid composition of the protein therefore influences the level of dye binding. The protein lysate was assumed to have similar

overall amino acid composition as the reference protein bovine gamma globulin (BGG).

Procedure:

- A dilution curve of 0, 1, 2, 3, 4 and 5 µg of standard protein was made by pipetting 0, 2, 4, 6, 8 and 10 µl of 0.5 µg/µl BGG in 3 parallels in a 96-well plate and adding H2O to 10 µl
- 1 µl of each lysate was pipetted on the plate in 3 parallels. H_2O to 10 µl was added.
- 100 µl of dye was added to each well
- After a minimum of 5 minutes incubation, the absorbance at 600 nm was read on a Modulus microplate spectrometer (Turner BioSystems)
  A standard curve for each plate was made in spreadsheet software. Protein concentrations in the samples were computed from the equation describing the curve.

2.7.3 Polyacrylamide gel electrophoresis of proteins

In electrophoresis, proteins or other macromolecules are separated based on size by the use of electric current. The secondary structures of the proteins are denatured by heat and the anionic detergent LDS (lithium dodecyl sulphate) to long polypeptide chains. Additionally, a reducing agent containing dithiothreitol (DTT, Cleland's reagent) reduces disulphide bridges in the protein. LDS binds to hydrophobic groups along the polypeptide, giving it a uniform negative charge that is proportional to the length of the protein. As the negative charges on LDS repel each other, the polypeptide is kept linear during the electrophoresis. When current is applied to the system, the negative charges are drawn towards the positive pole.

The gel consists of a highly cross-linked polyacrylamide matrix. Longer peptide chains are hindered by the matrix to a higher degree than shorter ones. This causes small proteins to travel faster towards the positive pole, thus separating the proteins based on size. [6]

LDS-PAGE (PolyAcrylamide Gel Electrophoresis) was done using the pre-cast Novex Midi Bis-Tris gel system (Invitrogen) by the protocol provided by the manufacturer.

Sample preparation

A maximum of 22 µg protein was prepared for electrophoresis by adding de-ionized H$_2$O to 6.5 µl, 2.5 µl NuPage sample buffer and 1 µl NuPage reducing agent (Bio-Rad), and heated at 70°C for 10 minutes on a heat block.

The well separator is removed from the gel, wells are rinsed with running buffer, and protective tape is removed from the bottom of the gel. The gel system is assembled and filled with running buffer (MOPS [3-(N-morpholino)propanesulfonic acid] 20 mM, ~7 dl) to the fill line. Samples are applied carefully in the wells along with a ladder of markers (1 kb dual-color ladder, Bio-Rad, 2.5 µl).

The electrophoresis is run on 180V until the marker proteins are sufficiently separated (~1 hr).

2.7.4 Western Blot

The gel matrix is unstable, and the separated protein spots need to be transferred to a more durable medium. This is accomplished using electric current. As in gel electrophoresis, the proteins carry a negative charge and will follow a current towards the positive pole. A membrane placed between the gel with samples and the positive pole retains the proteins but allows the buffer through. The protein spots adhere to the membrane in the same pattern as they were in the gel, as illustrated in figure 2.8.

Proteins were transferred from the gel matrix to a nitrocellulose membrane with 0.2 µm pore size using dry blotting (iBlot, Invitrogen) for 9 minutes.
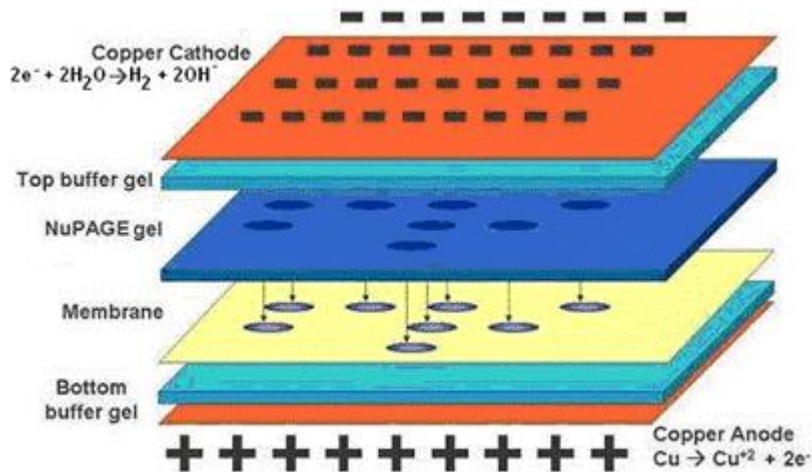
Figure 2.8: Protein blotting set-up (Invitrogen).

2.7.5 Antibody staining

Antibodies are found in all vertebrates as part of the adaptive immune system. These small proteins bind specifically to epitopes (small motives, typically 5-6 amino acids) on an antigen, which can be any foreign substance, usually protein. Each antibody molecule has two identical antigen binding sites, each consisting of parts of the variable region of the light and heavy chain (see figure 2.9). The great versatility of the antibody specificities stem from the random recombination of the DNA sequence coding for the variable region. In the heavy chain, 4 gene segments are selected from a total of 87. A similar recombination happens in the gene for the light chain. This random selection of segments ensures an enormous diversity in the specificities of antibodies. A screening process in the bone marrow and thymus removes autoreactive antibodies that bind to innate structures of the body. The high specificity of the antibody binding makes them well suited for detection of specific proteins.

Polyclonal antibodies are raised in mammals by injecting the antigen. The animal, e.g. a mouse, will produce antibodies against the antigen as part of its immune response against the foreign substance. The antibodies can later be isolated from the blood plasma and purified using affinity chromatography. Secondary antibodies are raised in another animal, e.g. a rabbit, using (in this example) mouse antibodies or parts thereof as the antigen. As the rabbit and mouse immunoglobulins differ in

structure, the rabbit interprets the antibodies of mouse origin as foreign and produces antibodies against them. After purification of rabbit-anti-mouse (RAM) antibodies specific for the constant regions of the mouse antibody, the secondary antibody is coupled to a detectable probe, commonly horseradish peroxidase (HRP) that can cleave a luminescent agent for detection. The RAM antibody can be used as a detector of any primary antibody raised in mouse. This two-step process lowers costs as the detection antibody can be produced in larger quantities more effectively than coupling all primary antibodies to probes. Polyclonal antibodies differ somewhat, as they arise from different B-cell clones and recognize different epitopes on the antigen.

Monoclonal antibodies are produced by immortalized hybridoma cells. All monoclonal antibodies from the same clone are identical. [80]
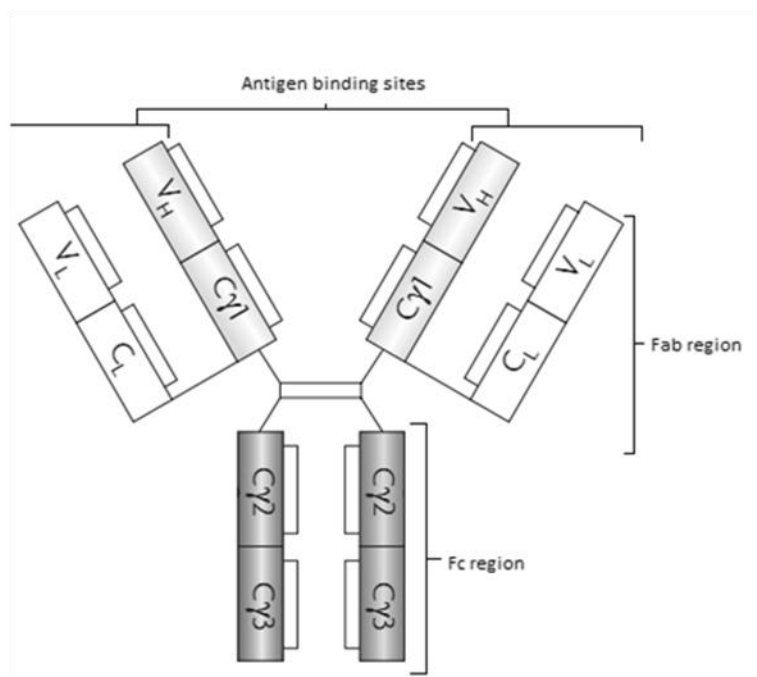
Figure 2.9: Schematic structure of IgG. Adapted from [81].

The antibody against S100A4 was purchased from Sigma and was raised in rabbit. The housekeeping gene α-tubulin was used as the loading control (antibody

purchased from Calbiotech, raised in mouse). Rabbit anti-mouse-HRP and goat anti-rabbit-HRP (Daco) were used as secondary antibodies in this study.

Procedure:

- The membrane is incubated in 50 ml 10% dry milk in 0.25% TBST buffer (w/v) for a minimum of 1 hour to saturate the protein binding membrane.
- Membrane is cut to give experimental and housekeeping genes on separate membranes
- Membranes are incubated with primary antibody diluted in 5% dry milk in 0.25% TBST buffer for a minimum of 1 hr or over night.

The primary antibody-milk mixture can be used up to 4 times within 2 months. If the mixture is stored, 15 µl Na-azid is added after the first use as a conservant.

2.7.6 Digital development

ECL (Enhanced ChemiLuminescence, Thermo Fisher) is cleaved by HRP, producing a luminescent signal that is detected by the digital chemiluminescence imager G:box iChemi (Syngene; Cambridge, UK) with the associated GeneSnap software. Pictures were typically taken with 1, 2, 5 and 10 minutes exposure time and saved as high-resolution image files (.tiff).

2.8 Cell viability assay

Transfection may induce reduction in cell viability, and optimizing of transfection protocols is usually performed to minimize unwanted cell death.

MTS (Owen's reagent; 3-(4,5-dimethylthiazol-2-yl)-5-(3-carboxymethoxyphenyl)-2-(4-sulfophenyl)-2H-tetrazolium) is a yellow-colored tetrazolium compound that is reduced in living cells to a purple formazan compound in the presence of the electron coupling agent phenazine methosulfate (PMS), measured as an absorption shift from

382 to 490 nm. The reaction is shown in figure 2.10. The reduction is presumed to be caused by the reducing agents NAPD and NAPDH. In dead cells, with no metabolic activity, these compounds are rapidly depleted and reduction of MTS ceases. The level of the Formazan product is interpreted as proportional to the number of viable cells. [82, 83]
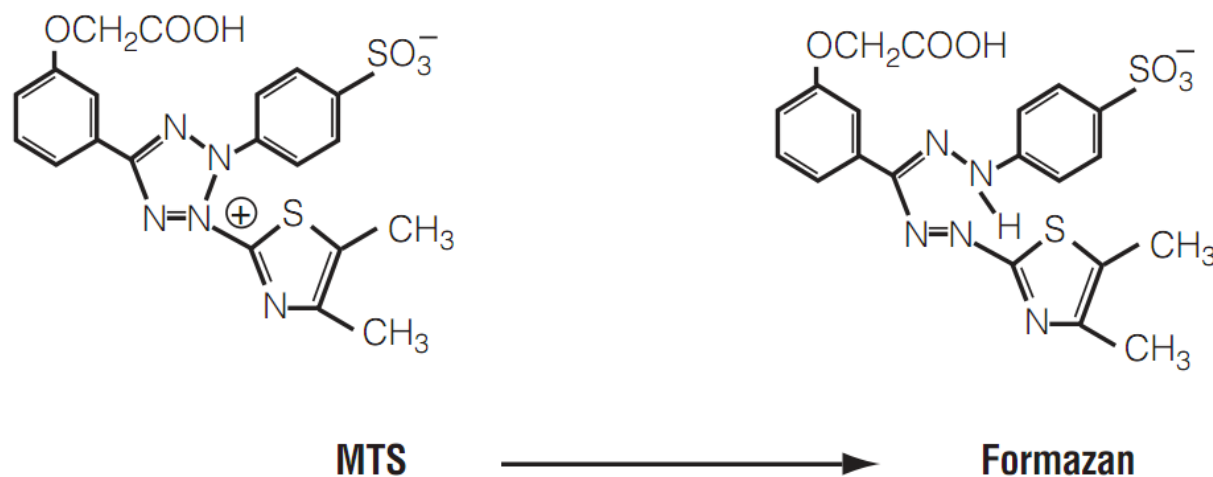
Figure 2.10: Structures of MTS and the Formazan product. [84]

In the present study, the CellTiter 96® AQ$_{ueous}$ One Solution Cell Proliferation Assay (Promega, Fitchburg, USA) was used to assess cell viability in transfected cells versus untreated cells by the following adapted protocol:

- Cells grown in 12-well plates were transfected with or without PCI treatment and incubated 20-24 hrs.
- A stock solution of 1:6 MTS in medium was made using 200 µl MTS solution in 1000 µl RPMI with added serum and L-glutamine.
- In dim light, 1 ml of the stock solution was added to each well. Untransfected cells were used as reference. A cell-free well (medium and MTS solution only) was used as a negative control.
- The plates were incubated without light for 1-3 hours until a dark purple-brown color could be observed in some wells. Aluminum foil was used to ensure dark incubation. Checks for color change were performed every 30-40 minutes in dim light.
- Absorption at 490 nm was quantified using a Victor 1420 spectrophotometer (Wallac, now PerkinElmer, Waltham, US). A$_{490}$ should fall within the linear area (~0.6 to 1.4). The absorption of the no-cell condition was subtracted from all

measurements. Viability of transfected cells was calculated as a percentage of the untransfected reference.

3. Results

3.1 Optimization of transfection protocol

3.1.1 Flow cytometry

Expression of EGFP protein after transfecting cells with EGFP mRNA was quantified using flow cytometry. Table 3.1 indicates the proportions of propidium iodide resistant (living) singlet cells among the 10 000 measured particles, as well as the percentage of EGFP expressing cells amongst singlet, PI negative cells, using PEI or cyclodextrin as the transfection agent, measured 24 hours after transfection.

Initially, a broad PEI-based assay was carried out (table 3.1a). N/P 5 produced the best efficiency, with 50.5% of the cells expressing the transfected mRNA as protein. The PCI targeting effect was demonstrated; the PCI+ conditions exhibited a high transfection rate, versus low expression in the PCI- conditions. In this design, the amount of dead cells and cell fragments increased with increasing N/P ratio. PCI treatment induced a further reduction in viability.

The transfection conditions that produced the best transfection rates in this assay (N/P 3, 5 and 7) were forwarded to further refinement.

When using β-6CDP (table 3.1b), only transfection rates up to 21% were obtained with the carrier concentrations assayed, with no additional effect from PCI treatment. Based on these results, it was decided to use PEI in the further studies of gene interactions. In this single-cell based study, transfection efficiency is of higher importance than cytotoxicity.

After multiple rounds of refining transfection conditions (number of cells seeded and incubation times) transfection efficiencies up to 69.4% were observed (table 3.1c). Again, N/P 5 produced the best efficiency with PCI. All flow cytometry assays were done in OHS cells.

Table 3.1: Fractions of viable cells (PI-) and EGFP positive cells after transfection, as determined by flow cytometry. (a) Initial PEI-based transfection, (b) β-6CDP-based, (c) PEI-based after optimalization. PI negative, single cells are given as percentage of the total number of measured particles. Relative survival is PI- in percent of PI- in control. EGFP positive cell count is given as percentage of PI negative, singlet cells. Each value is the mean of measurements of two individual samples. Values marked with * are based on one sample. 10 000 events were recorded per sample. All measurements were done in OHS cells.

PEI	mRNA	N/P ratio	PCI	PI- (%)	Relative survival	EGFP+ (%)
0	0	Control	-	51.5	100.0	1.5
			+	49.8*	96.8	1.4*
0.20 µg	1 µg	1.5	-	55.6	108.1	3.4
			+	45.6	88.6	26.7
0.41 µg	1 µg	3	-	54.7	106.3	2.7
			+	50.4	98.0	42.2
0.68 µg	1 µg	5	-	49.2	95.5	4.4
			+	37.2	72.2	50.5
0.95 µg	1 µg	7	-	38.7	75.1	5.1
			+	34.4	66.9	45.2
1.22 µg	1 µg	9	-	34.0	66.1	5.7
			+	27.3	53.0	26.2
1.50 µg	1 µg	11	-	34.2	66.5	8.8
			+	33.3	64.7	19.0

a)

β-6CDP	mRNA	PCI	PI- (%)	Relative survival	EGFP+ (%)
0	0	-	57.0	100	2.8
		+	54.6	95.8	2.5
12.5 µg	1 µg	-	33.6	58.9	14.6
		+	35.3	61.9	13.5
25 µg	1 µg	-	28.9	50.7	21.4
		+	31.6	55.4	15.3
50 µg	1 µg	-	31.2	54.8	18.0
		+	33.4	58.6	19.7

b)

PEI	mRNA	N/P ratio	PCI	PI-, %	Relative survival	EGFP+, %
0	0	Control	-	54.5	100.0	0.6
			+	51.2	93.9	0.4
0.41 µg	1 µg	3	-	50.9	93.4	2.8
			+	37.7	69.2	61.9
0.68 µg	1 µg	5	-	49.8	91.4	7.3
			+	29	53.2	69.4
1.09 µg	1 µg	8	-	52.5	96.3	6.9
			+	11.6	21.3	64.5

c)

3.1.2 Microscopy

Viewing EGFP transfected cells in a microscope gives an overview of transfection efficiencies and cell survival. Figure 3.1 shows EGFP expression in cells when viewed at 20x magnification in a fluorescence microscope using a 488 nm filter. In transfections using N/P ratios 5 and 10 (left, middle), high transfection rates were observed in the PCI treated samples, while few non-PCI-treated cells had taken up the gene. In the N/P 15 transfection, a considerable number of cells took up the gene without the aid of PCI ("leakage"). In the N/P 15 PCI-assisted transfection, several dead or dying cells are observed as circular spots.
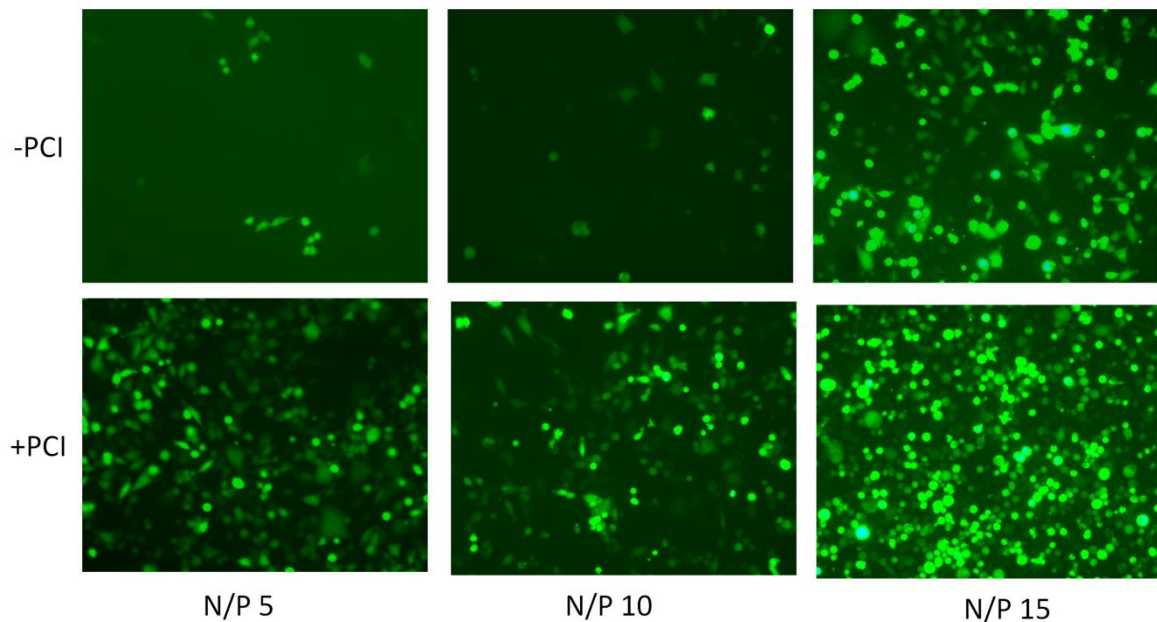
Figure 3.1: EGFP transfected OHS cells viewed at 20x magnification 24 hours after transfection. Top panels are transfected without the use of PCI, bottom panels are PCI treated.

3.2 Measurements of S100A4 delivery

Once an efficient protocol for PEI-mediated, non-PCI mRNA delivery was established, delivery of S100A4 was confirmed on the mRNA and protein level. The parameters used for the transfections assessed in this section are listed in table 2.1.

3.2.1 RNA analysis

Quantitative real-time PCR (qPCR) of RNA isolated from transfected cells 24 hours after transfection confirms successful delivery of S100A4 mRNA into cells, as shown in figure 3.2. The amount of S100A4 recovered from the cells is higher in the samples that received a higher dose of S100A4 mRNA in the transfection. The lowest expression value within each graph is set to 1. C_t values are listed in appendix A.

a)
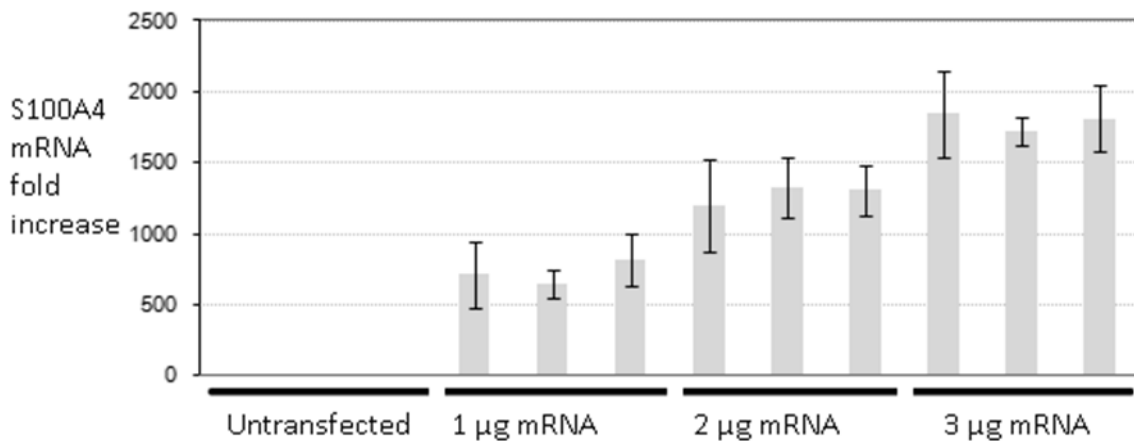
b)
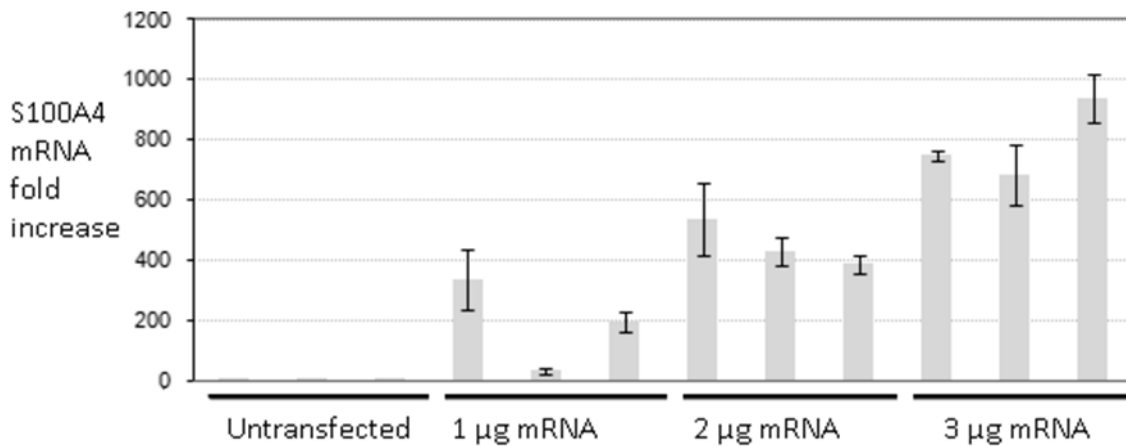
Figure 3.2: Relative expression of S100A4 mRNA in (a) LOX and (b) OHS samples treated with 0, 1, 2 or 3 µg S100A4 mRNA combined with 3 µg PEI, as detected by qPCR. 3 individual samples are shown for each dosage, with 2 replicate measurements per sample. Untreated controls are set to 1. Error bars denote standard deviation. Note that the expression scales differ between the cell lines.

3.2.2 Protein expression analysis

Western blots

Western blots confirm expression of S100A4 protein 24 hours after transfection, as presented in figure 3.3. In LOX cells (fig 3.3a), results showed that transfection using 1 μg S100A4 mRNA produced relatively weak bands, 2 μg mRNA produced slightly brighter bands, while the strongest bands were found when using 3 μg S100A4 mRNA. Of note, no band was visible in the untransfected cells in agreement with the fact that the LOX cell line is negative for S100A4 expression.

In the OHS cell line (fig 3.3b), the protein level of S100A4 was more challenging to quantify due to the high innate S100A4 expression. Our results showed that all experimental groups exhibited a high level of S100A4 protein. An upregulation may be masked by the difference in protein loading as visible from the loading control.
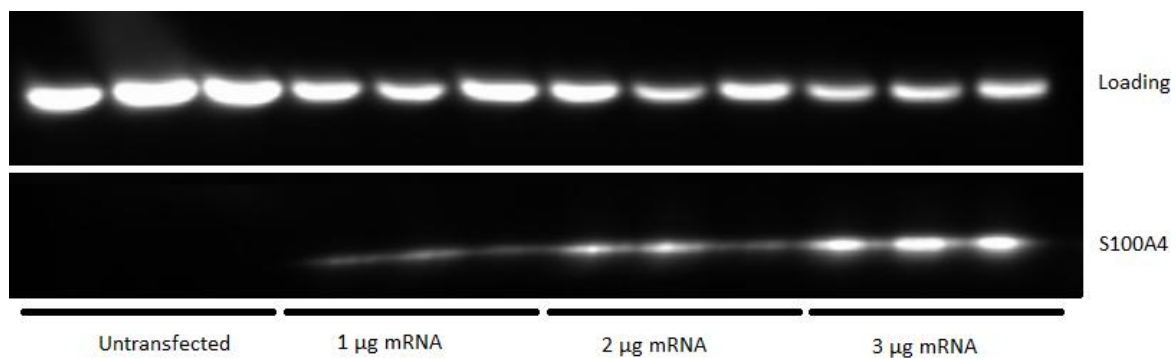
a)
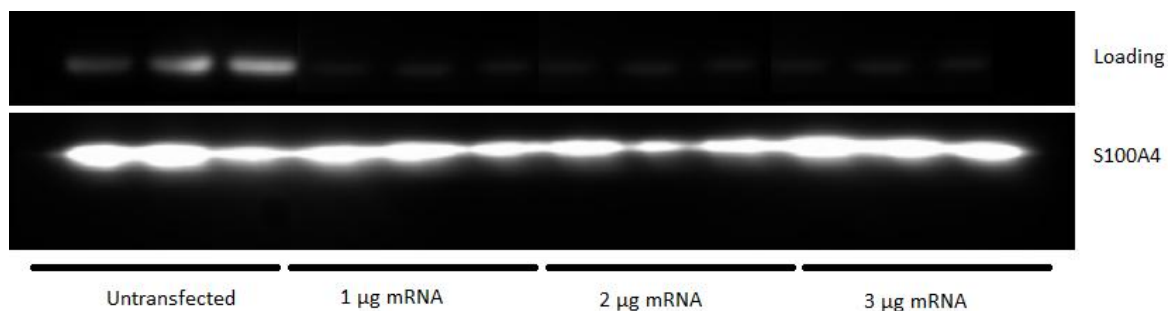
b)

Figure 3.3: Western blots of S100A4 (bottom) and α-tubulin (indicator of loading volume; top) in (a) LOX and (b) OHS cells. Three individual replicates for each condition were blotted in the same blot. Lanes 1 to 3 from right to left: Untransfected cells. Lanes 4 to 6: 1 μg S100A4 mRNA. Lanes 7 to 9: 2 μg S100A4 mRNA. Lanes 10 to 12: 3 μg S100A4 mRNA.

3.3 Target gene expression analyses

3.3.1 Expression microarray profile

A clustering analysis was done on the expression profile as a quality check, as shown in figure 3.4. Samples that received identical treatment are expected to cluster together. One sample of EGFP transfected LOX cells was excluded from further analyses due to clustering differently than the rest of the samples from the LOX cell line. Therefore, the S100A4 treated LOX samples were compared to a baseline consisting of only one sample.
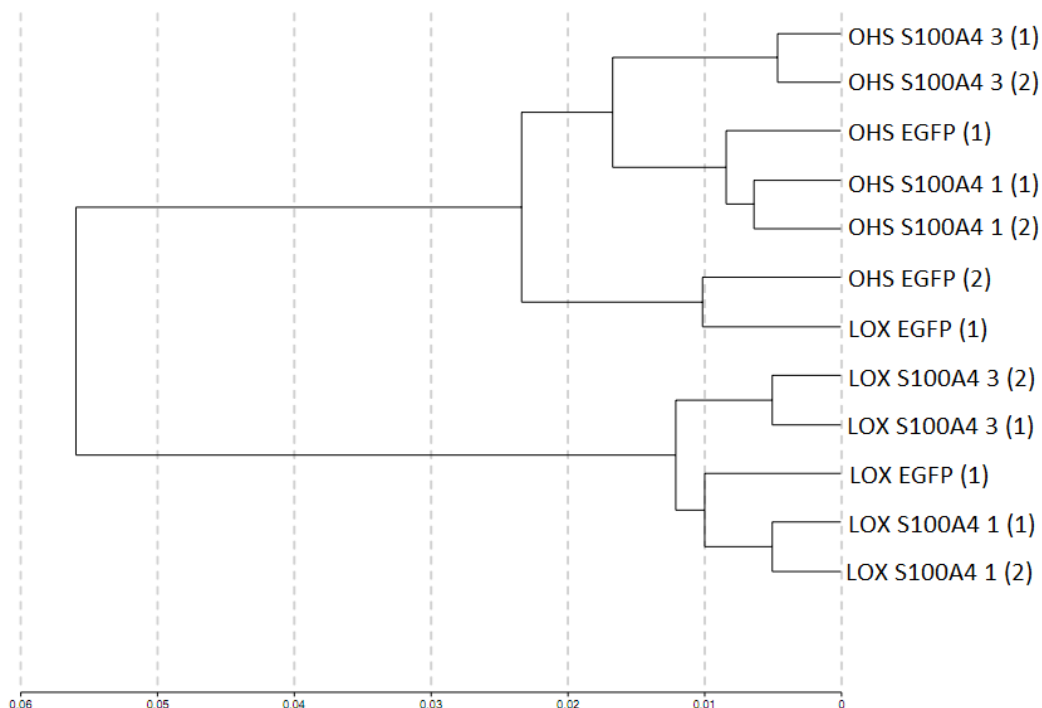
Figure 3.4: Samples clustered based on similarity in expression pattern. The sample labeled LOX EGFP (1) clustered together with the OHS samples and was excluded from further analyses.

To identify differentially expressed genes, the Rank Product analysis [74] was employed with a q-value cut-off of 0.05. Top results of these analyses are shown in table 3.2.

Table 3.2: Rank Product of control versus transfected samples for both cell lines combined (a), OHS (b), (c), and LOX (d), (e). Genes in boldface were selected for further validation of differential expression.

a) Control vs 3 µg, both cell lines combined

Rank	Probe ID	Gene symbol	Fold change	q-value
1	3240216	**SNORA71C**	30.514	0.000
2	2172933	**LCN12**	4.244	0.023
3	1803302	**CRK**	4.201	0.045

b) Control vs. 1 µg, OHS

Rank	Probe ID	Gene symbol	Fold change	q-value
1	3240216	**SNORA71C**	35.461	0.000
2	1775501	IL1B	10.210	0.010
3	2172933	**LCN12**	5.210	0.038

c) Control vs. 3 µg, OHS

Rank	Probe ID	Gene symbol	Fold change	q-value
1	3240216	**SNORA71C**	39.417	0.000
2	2172933	**LCN12**	4.969	0.046

d) Control vs. 1 µg, LOX

Rank	Probe ID	Gene symbol	Fold change	q-value
1	1684306	S100A4	57.743	0.000
2	1688780	S100A4	4.822	0.014
3	1681332	**LOC646496**	3.245	0.017
4	1713934	LITAF	3.462	0.018
5	1779448	EFHD1	3.367	0.027
6	2355559	PSAP	2.312	0.032
7	1703430	FLJ10374	2.313	0.034
8	2326712	BACE2	2.507	0.034
9	2104356	**COL1A2**	2.911	0.045

e) Control vs 3 µg, LOX

Rank	Probe ID	Gene symbol	Fold change	q-value
1	1684306	S100A4	63.827	0.000
2	1681332	**LOC646496**	41.968	0.001
3	2384544	**ADAM15**	7.253	0.005

A set of six genes which had high ranks (below the q=0.05 threshold in at least one comparison) and were relevant for cancer progression were selected for wet-lab validation. The expression pattern of the chosen candidate genes in the array are shown in table 3.3.

Table 3.3: Expression and fold change for candidate genes in control and treated samples. Expression values are quantile normalized and given as the mean of two parallel samples, except for the EGFP control in LOX which is only one measurement. Fold change calculation was done in J-express.

Gene symbol	Cell line	Control	Treated (1 μg)	Treated (3μg)	Fold change 0 vs 1	Fold change 0 vs 3
CRK	OHS	283.968	79.010015	76.798825	-9.21	-9.76
	LOX	579.116	90.885745	76.41251	14.26	10.07
Col1a2	OHS	5570.01	6518.362	5283.989	1.42	-1.17
	LOX	74.3293	261.05825	92.13798	629.77	79.07
ADAM15	OHS	636.231	1376.4135	2922.826	4.66	21.12
	LOX	132.418	197.25945	961.7767	680.38	148.25
LCN12	OHS	477.8	89.35013	93.660365	-27.14	-24.69
	LOX	293.708	85.221255	94.46966	24.7	30.4
SNORA71C	OHS	3101.2	86.27864	77.51149	-1257.46	-1553.71
	LOX	1542.52	124.094315	83.27928	9.19	4.36
LOC646469	OHS	133.5	1990.1535	5248.549	251.96	1740.25
	LOX	71.0238	231.14745	3000.886	747.74	125080.76

Overrepresentation analysis

A list of 100 top differentially expressed genes was obtained using Rank Product for control versus 3 μg treated samples in both cell lines combined, ignoring hypothetical and predicted genes that are not recognized by the overrepresentation analysis tool. When comparing this list to a random human reference using the web application DAVID, Gene Ontology (GO) terms associated with the extracellular space were significantly overrepresented, as shown in table 3.4.

Table 3.4: Screenshot from DAVID software, showing the four most significantly overrepresented Gene Ontology terms associated with the set of 100 top ranked genes from the expression profile of OHS and LOX cells combined.

Term	Genes	Count	%	P-Value	Benjamini
extracellular region part		20	21.3	7.4E-7	1.1E-4
Secreted		23	24.5	7.7E-6	1.5E-3
extracellular space		15	16.0	2.0E-5	1.4E-3
extracellular region		26	27.7	4.4E-5	2.1E-3

3.3.2 qPCR validation

Figure 3.5 summarizes the result of qPCR using primers for candidate genes from the expression microarray. C_t values are listed in appendix B. The graphs to the right show the intensities in the microarrays for comparison.

e)
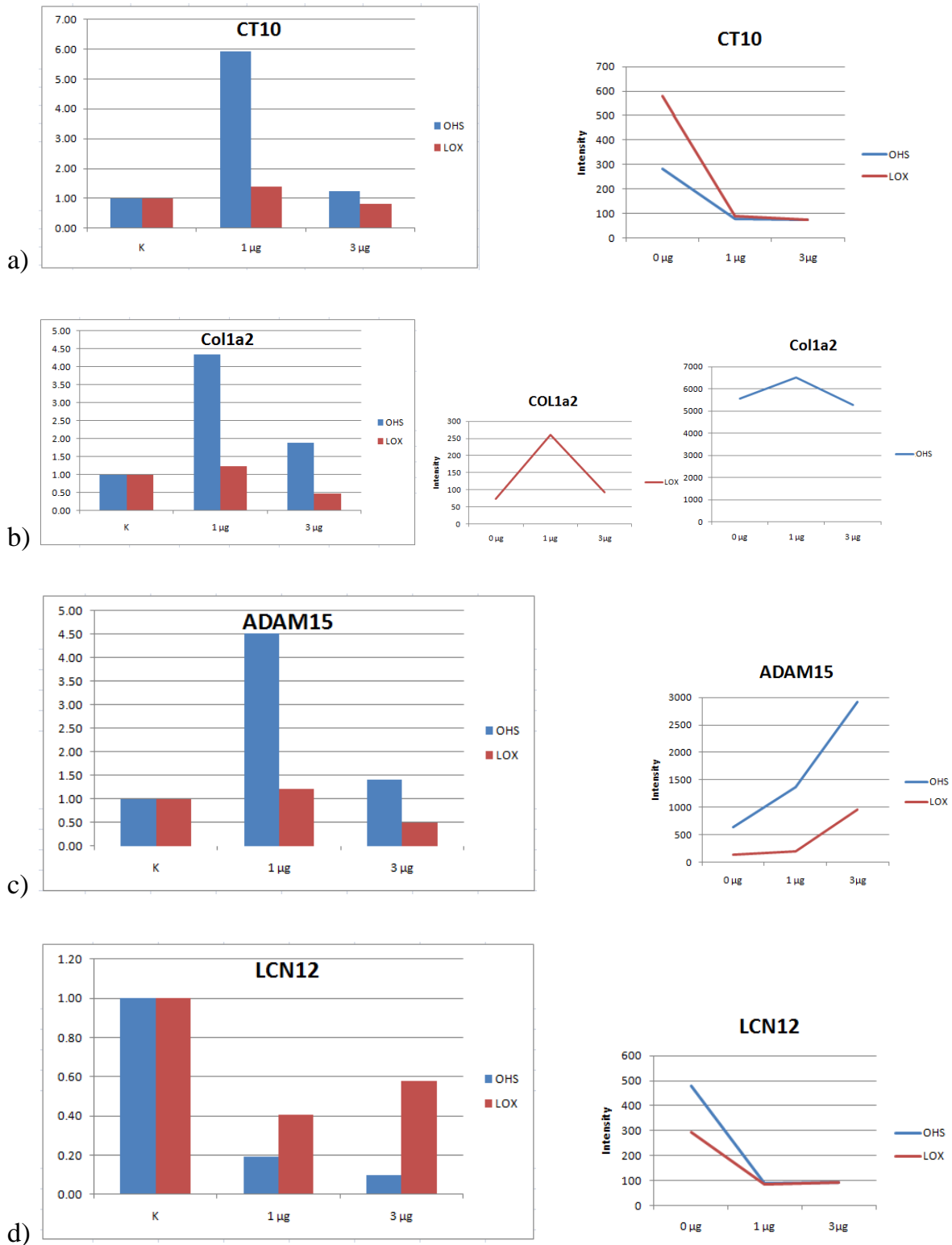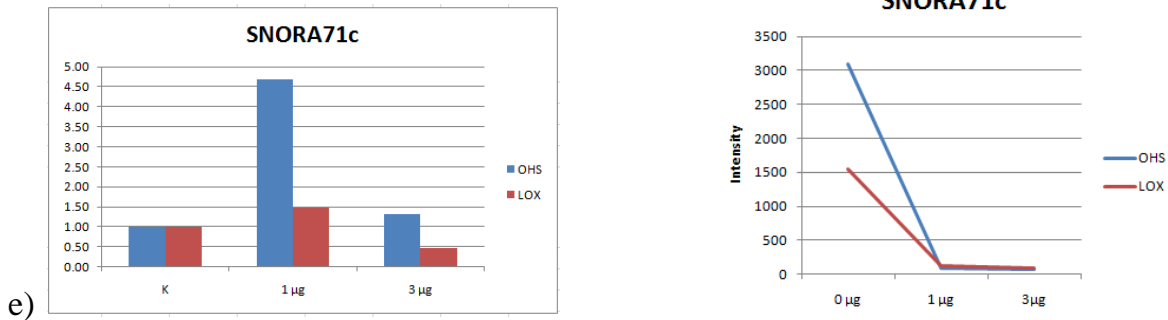
Figure 3.5: Relative expression of (a) CT10, (b) Col1a2, (c) ADAM15, (d) LCN12, (e) SNORA71c and (f) LOC646469 as determined by qPCR. The second axis shows the fold change. Expression in EGFP transfected samples (K) is set to 1. Each bar represents the average of 3 individual experiments for LOX, and 2 individual experiments for OHS. Graphs showing the intensity for each of the genes in the microarray analysis are included on the right side for comparison.

CT10 did not pass qPCR validation.

Col1a2 did show a similar expression pattern in the qPCR as in the microarray, however the magnitude of the changes deviated: LOX cells had a 23% increase followed by a 2.5 fold decrease in the qPCR (microarray: 3 fold increase followed by 2.8 fold decrease). OHS cells had a 4.35 fold increase followed by a 2.3 fold decrease (microarray: 15% increase followed by a 19% decrease). Further validation would be necessary to establish whether Col1a2 really is regulated by S100A4.

 ADAM15 did not pass qPCR validation.

LCN12 downregulation was confirmed by qPCR validation. In LOX, the decrease in expression was about one fold between control and treated samples combined (microarray: three fold decrease). In OHS, the decrease was about seven fold (microarray: five fold decrease).

SNORA71c did not pass qPCR validation.

Validation of LOC646469 was attempted, but was unsuccessful, likely due to primer dimerization.

3.3.3 Primer validation by electrophoresis of transcripts

Shown in figure 3.6 are qPCR transcripts separated by gel electrophoresis. Expected transcript lengths are found in Appendix C. Observed transcript lengths are in good accordance with expected lengths. A smear at about 25 bp is visible for LOC646469, indicative of erroneous transcripts.

Figure 3.6: DNA electrophoresis gel picture showing the lengths of qPCR transcripts. Theoretical transcripts lengths in basepairs: CT10: 95, Col1a2: 62, ADAM15: 77, LCN12: 73, SNORA71c: 80, LOC646469: 66, S100A4: 79, TBP: 64, RPLP0: 64
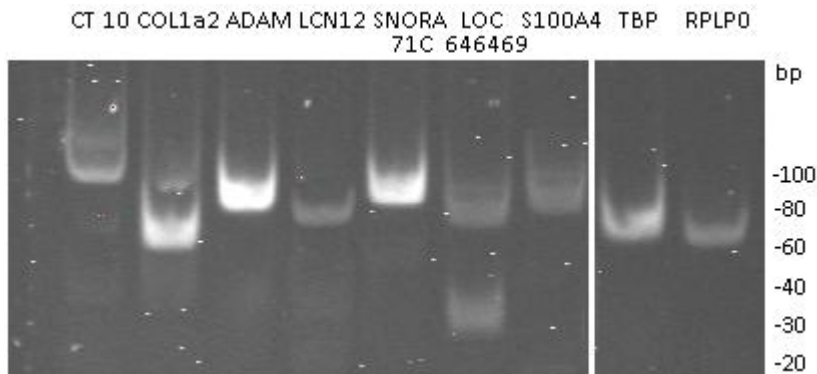
3.4 Particle size measurements

Particle sizes after complexion of mRNA and PEI using different mRNA concentrations were measured using a Malvern Zetasizer. 1, 2 and 3 µg S100A4 mRNA complexed with 3 µg PEI corresponding to N/P 22, 11 and 7.3 respectively, was measured starting after 30 minutes. Results are shown in table 3.5.

Table 3.5: Sizes of transfection particles in nm (largest peak).

	1 µg mRNA	2 µg mRNA	3 µg mRNA
Measurement 1	315.4	584.2	430.2
Measurement 2	375.4	518.1	429.4
Measurement 3	438.7	502.2	759.0
Mean:	**376.5**	**534.8**	**539.5**

There was considerable variation in the measured particle sizes. Incubation time was observed to be an important factor for particle size; when incubated for 60 minutes, particle sizes up to 1000 nm were observed. Further details are listed in Appendix D. β-CDP-based particles were too polydisperse to be measured with this equipment.

3.5 Cell viability assays

Cell viability was assessed using the MTS assay 20 hours after mRNA transfection using parameters listed in table 2.1 with and without PCI treatment. In the non-PCI transfection, a 10% reduction in cell viability is observed in the LOX cell line in the 1 μg transfection, which has the highest positive charge. This reduction becomes smaller in the higher mRNA conditions, which have a more neutral charge. No reduction in cell viability was observed in the OHS line.

In the PCI-assisted transfections, a 25-30% reduction in viability was observed for the higher N/P ratios in the assay when compared to the same transfections without PCI treatment. In the lowest ratio in the assay, the viability difference between PCI and non-PCI is negligible. The results are presented in figure 3.6.
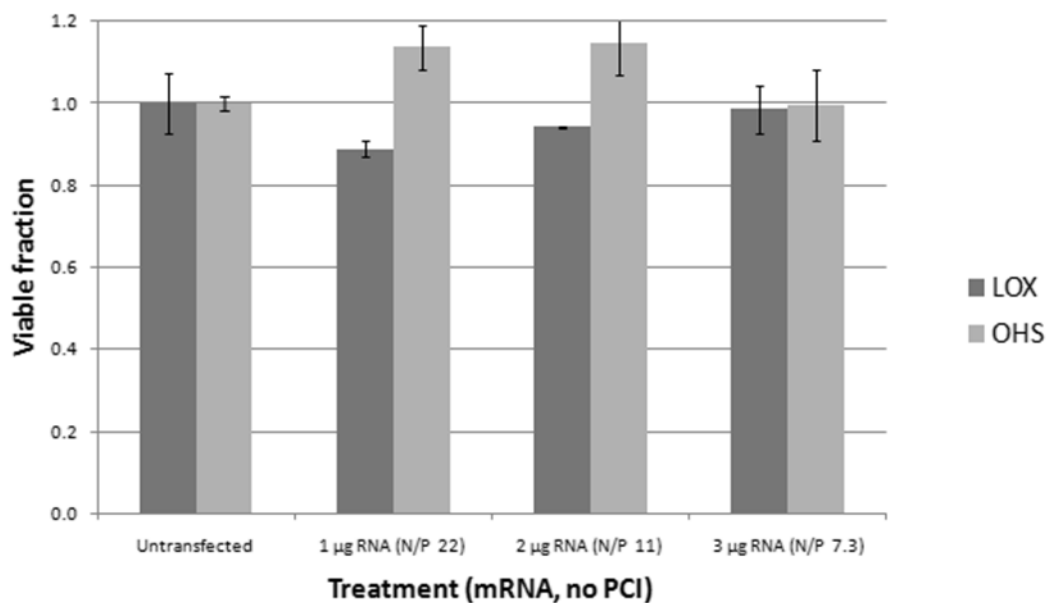
a)
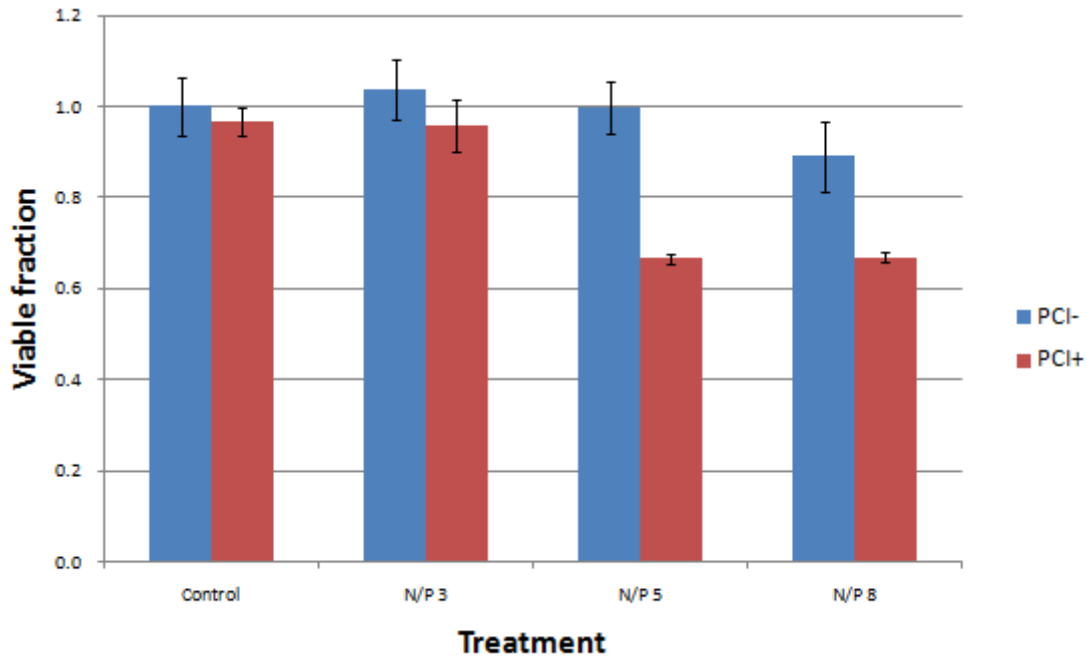
b)

Figure 3.6: Cell viability after transfection. a) Without PCI treatment, conducted in LOX and OHS cells using fixed concentrations of PEI with varying concentrations of mRNA. b) PCI assisted transfections conducted in OHS cells with fixed concentrations of mRNA and varying concentrations of PEI. Each bar is the average of three different transfections. The error bars show the standard deviation.

4. Discussion

4.1 Gene therapy and transfection

4.1.1 Methodical considerations

An mRNA-based upregulation study can be regarded as the opposite of a siRNA downregulation study, using the same set of procedures to influence the gene expression of cells in two opposite ways. A few notable differences exist; siRNA are easily synthesized and commercially available in contrast to mRNA molecules. siRNA molecules consist of two short double mRNA strands (19-21 bp), while mRNA transcripts are single stranded and much longer. The size difference of the molecules will naturally influence the formation of transfection complexes, as discussed below.

The two cell lines chosen for the study are quite different, most strikingly in terms of endogenous S100A4 expression, but also in cell type origin. LOX is an amelanotic melanoma line derived from melanocytes of the skin, while OHS is an osteosarcoma cell line derived from retinoblastoma origin. It is therefore expected that the cell lines have different expression patterns, in addition to different endocytotic capacity.

Flow cytometry was used in the initial part of the project, to assay a broad range of transfections designed for use with PCI. PCI directed transfection was demonstrated. In the rest of the study, transfections designed for use without PCI were employed. For this, a PEI concentration just above the point where leakage occurs was identified. The high PEI concentrations for use without PCI were not investigated using flow cytometry, but delivery and protein expression were instead confirmed using qPCR and Western blotting.

β-6CDP has been shown to be effective with siRNA, [34] but performed poorly with mRNA. Other transfection agents also deliver siRNA better than mRNA (unpublished results from the research group of E. Hovig). This could be because siRNAs are shorter, giving more options for the conformation of complexes. In

support of this hypothesis, the Zetasizer was unable to measure the size of the β-6CDP-based complexes due to high polydispersity.

4.1.2 Internalization mechanisms

Both PEI- and β-6CDP-based complexes are cationic and are theorized to adhere to the cell based on electrostatic interactions. β-CD is additionally hypothesized to bind cholesterol on the plasma membrane. [32] The adhesion to cholesterol would require the particle to be in direct contact with the plasma membrane, which seems unlikely knowing the cell surface is covered with carbohydrate chains.

The transfection particles range from 370 to 540 nm. The literature is conflicting regarding which mechanisms of endocytosis are at play for particles in this size range. [45, 85] It is difficult to determine internalization mechanisms in blocking studies, as the involved genes tend to act in more than one pathway.

RNA is easily degraded. Though it is to a degree protected by the complexation agent, it must exit the endocytic pathway at an early stage to reach the cytosol in an intact state, as the environment gets progressively more degrading as the endosomes mature. The timespan from a material is endocytosed until it reaches the lysosomes is highly variable, often in the range of ~5 to 30 minutes depending on which pathway is employed [86]. In PCI-based trials with a 4 hrs chase, the material that was endocytosed shortly after adding the complexes to the cells, have reached the lysosomes long before the light treatment. The complexes that are released in the light treatment were endocytosed in the latter part of the chase. This means there needs to be enough transfection complexes to uphold a high internalization rate throughout the chase period.

In non-PCI, proton sponge based transfections, the swelling is dependent on the acidification of endosomes, giving continuous release to the cytosol for as long as transfection complexes are endocytosed or until cells are harvested. This may give

more mRNA to each cell than the light-directed transfection which gives release from endosomes at only one time point.

4.2 Microarray experiment

4.2.1 Methodical considerations

The microarray experiment included two biological replicates of each experimental condition. The parallels were prepared on the same days, from different cell culture plates. Two biological parallels are considered to be few in the context of microarrays; 4 to 5 are recommended. With fewer replicates, expression changes need to be larger in order to be detected in the statistical analysis. It is important to determine whether the analysis gives reliable results for groups of two parallel samples. With a lower number of parallel samples, the experiment is also vulnerable if a sample does not pass post-experiment quality controls, as was the case in the LOX control condition in this study. Additionally, the data are expected to have a relatively high degree of noise because the samples consist of a mixture of affected and unaffected cells.

The control condition was transfected using the same parameters as the experimental condition, but with EGFP mRNA in place of S100A4 mRNA. These samples are expected to have unspecific expression changes caused by the transfection itself, but no specific expression changes caused by the transfected gene as EGFP is foreign to human cell lines. This gives a baseline from which the specific changes can be seen. Two concentrations of S100A4 mRNA were used in order to be able to determine a dose-response relationship.

It should be noted that the mRNA transcriptome as detected by expression microarray profiles are not necessarily analogous to the protein expression of the cell, due to regulatory mechanisms in the translation step (as reviewed in [87]).

4.3 S100A4 gene interactions

4.3.1 Selection of candidate interacting genes

The expression profiling identifies genes whose expression is influenced by the presence of S100A4. It does not distinguish between direct interactions (e.g. S100A4 acting as an activator of transcription) and indirect interactions (e.g. S100A4 influencing the activity of another transcription factor). A significant difference in the profile is therefore not proof of a direct interaction between S100A4 and the affected gene.

Microarray data are inherently noisy, and it is not always possible to distinguish real signals from noise. Therefore, results obtained in a microarray experiment should always be validated using qPCR or Northern or Western blotting. [87] For low-frequency genes, the methodical noise is larger. [88]The genes selected for validation of differential expression were among the genes that showed the most significant differential expression in the microarray profile, as shown in table 3.2. Some of the selected candidate genes were present at a quite low frequency, and difficulties in validation were therefore expected. These genes were nevertheless forwarded to wet-lab validation due to interest in their biological function.

Candidate interacting genes: Validation

Two of the five successfully amplified candidate genes passed qPCR validation. This is low, considering the significant differential expression of all candidates in the microarray (all were picked from rank product lists with q<0.05). This analysis does not take into account the magnitude of the intensity in the microarray. Probes with low intensities, such as CT10, have a larger variation because of a lower pool of transcript in the amplified sample. [88]

Additionally, the hypothetical gene LOC646469 was not successfully amplified in qPCR. This sequence is somewhat repetitive, and we were therefore unable to design primers with no self base pairing.

4.3.2 Interacting genes

Of six candidate interacting genes two were confirmed to be influenced by S100A4 expression, three failed to validate and one was not validated due to methodical difficulties.

LCN12

The gene LCN12, coding for the transporter lipocalin 12, was shown to be transcriptionally regulated by S100A4.

The lipocalins derive their name from greek; *lipos*, meaning fat, and *calyx*, meaning cup. This diverse family of small, mainly secreted carrier proteins in the calycin superfamily is found in eukaryotes and eubacteria. [89] The proteins have an eight-stranded beta barrel forming the cup-shaped cargo binding site, in addition to binding to specific cell-surface receptors and the ability to form complexes with other proteins via its loop domain. Lipocalins are implicated in a number of biological processes including retinoid binding, cancer cell interactions, maintenance of homeostasis, and immune response. Cargo include steroid hormones, retinoids, and lipids, all of which are small, hydrophobic molecules. The lipocalin binds specific receptors on the cell surface, either to be endocytosed or releasing its cargo which migrates passively through the plasma membrane. [90]

Several of the lipocalins have protease inhibitor activity, contributing to the cancer relevant part of their function, interfering with the migratory ability of the cancerous cell. [91]

Lipocalin 12 [92] is normally expressed in the epididymis in response to androgen stimulation, and *ex situ* expression is reported in several cancers. While not completely characterized, is proposed to act in the transport of retinoic acid to the retinoid receptor. [93]

Col1a2

This subunit of type I collagen was upregulated in samples treated with a low dose of S100A4 mRNA, but not in those receiving a high mRNA dose. This surprising pattern was recurring in both cell lines studied, consistent in the microarray and qPCR. Interfering with the extracellular matrix, including collagen, is an important part of the cell invasion process in the metastatic cascade, and type I collagen is dysregulated in a range of cancers. A study found induction of a matrix protease by type I collagen. [94]

LOC646469

This hypothetic gene showed the largest fold change among all genes in the microarray experiment and was therefore included in the qPCR validation although its function is unknown. The sequence lacks introns, and samples were therefore treated with DNAse to remove any genomic material before qPCR analysis. qPCR data show that the amplification reached C_t very late, if at all, indicative of quality issues with primers which was also confirmed by electrophoresis of qPCR fragments. There is a chance of DNA contamination in the RNA used in the microarray experiment as this RNA was not treated with DNAse, this does however not explain the large increase in measured LOC646469 expression in treated samples.

Overrepresentation analysis

The overrepresentation of several terms associated with the extracellular space within the list of genes affected by S100A4 expression, is in accordance with earlier findings linking S100A4 to metastasis.

4.4 Validations and quality controls

The efficacies of the transfections were confirmed on the mRNA and protein levels.

The timescale of the study did not allow for validation of candidate target genes on the protein level.

The use of two cell lines; one cell line with innate S100A4 expression and one completely lacking it, adds broadness to the study.

Cell viability: The data suggest that the LOX cell line is more sensitive to positive charge than OHS. PCI treatment in transfection enhances uptake of mRNA, but also increases cell death due to increased membrane rupture.

4.5 Conclusions

A technique for mRNA transfection was refined to give good transfection efficacy while keeping high cell viability.

S100A4 tranfection influences a range of genes, among which genes associated with the extracellular space are overrepresented.

The transporter protein lipocalin 12 is a target gene of S100A4. To our knowledge, this relationship has not been reported before. Additionally, the collagen precursor Col1a2 transcription appears to be influenced by S100A4.

References

1.   Barrow, M., *Portraits of Hippocrates.* Medical History, 1972. **16**(1): p. 85-88.
2.   Boyle, P. and B. Levin, *World Cancer Report 2008.* 2008, International Agency for Research on Cancer (IARC), WHO.
3.   *The Global Burden of Disease: 2004 update.* 2008, World Health Organization: Geneva.
4.   *40 Years of the War on Cancer.* Editorial, Science 2011. **311**(6024): p. 1540-1544.
5.   Vilenchik, M. and A. Knudson, *Inverse radiation dose-rate effects on somatic and germ-line mutations and DNA damage rates.* PNAS, 2000. **97**(10): p. 5381-5386.
6.   Alberts, B., et al., *Molecular Biology of the Cell.* Chapter 20. 2008, Garland Science: New York.
7.   Calabrese, P., S. Tavare, and D. Shibata, *Pretumor Progression: Clonal Evolution of Human Stem Cell Populations.* American Journal of Pathology, 2004. **104**(4): p. 1337-1347.
8.   Hanahan, D. and R. Weinberg, *The Hallmarks of Cancer.* Cell, 2000. **100**(1): p. 57-70.
9.   Weinberg, R.A., *The Biology of Cancer.* 1 ed. 2007, New York: Garland Science.
10.   Estreller, M., *Epigenetics in Cancer.* New England Journal of Medicine, 2008. **358**: p. 1148-1159.
11.   Griesenbach, U. and E. Alton, *Current status and future directions of gene and cell therapy for cystic fibrosis.* BioDrugs, 2011. **25**(2): p. 77-88.
12.   Benabid, E., *Gene therapy for Parkinson's disease: do we have the cure?* Lancet Neurology, 2010. **9**(12): p. 1142-1143.
13.   Sah, D. and N. Aronin, *Oligonucleotide therapeutic approaches for Huntington disease.* J Clin Invest, 2011. **121**(2): p. 500-507.
14.   Cavazzana-Calvo, M., et al., *Gene therapy of human severe combined immunodeficiency (SCID)-X1 disease.* Science, 2000. **288**: p. 669-672.
15.   Shirakawa, T., *The current status of adenovirus-based cancer gene therapy.* Molecules and Cells, 2008. **25**(4): p. 462-466.
16.   Nicolas, F., et al., *Silencing human cancer: identification and uses of microRNAs.* Recent Patents in Anticancer Drug Discovery, 2011. **6**(1): p. 94-105.
17.   Mu, L., et al., *Immunotherapy with allotumour mRNA-transfected dendritic cells in androgen-resistant prostate cancer patients.* British journal of cancer, 2005. **93**: p. 749-756.
18.   Toscano, M., et al., *Physiological and tissue-specific vectors for treatment of inherited diseases.* Gene Therapy, 2011. **18**(2): p. 117-27.
19.   Demeneix, B., et al., *Gene transfer with lipospermines and polyethylenimines.* Advanced Drug Delivery Reviews, 1998. **30**(1-3): p. 85-89.

20. Otmane Boussif, et al., *A Versatile Vector for Gene and Oligonucleotide Transfer into Cells in Culture and in vivo: Polyethylenimine.* Proc. Natl. Acad. Sci. USA, 1995. **92**: p. 7297-7301.

21. Moghimi, S., et al., *A two-stage poly(ethylenimine)-mediated cytotoxicity: implications for gene transfer/therapy.* Molecular Therapy, 2005. **11**: p. 990-995.

22. Hunter, C., *Molecular hurdles in polyfectin design and mechanistic background to polycation induced cytotoxicity.* Advanced Drug Delivery Reviews, 2006. **58**(14): p. 1523-1531.

23. Bøe, S., A.S. Longva, and E. Hovig, *Evaluation of Various Polyethylenimine Formulations for Light-Controlled Gene Silencing using Small Interfering RNA Molecules.* Oligonucleotides, 2008. **18**(2): p. 123-132.

24. Bøe, S., S. Sæbøe-Larssen, and E. Hovig, *Light-induced gene expression using messenger mRNA molecules.* Oligonucleotides, 2010. **20**(1).

25. Boussif, O., et al., *A Versatile Vector for Gene and Oligonucleotide Transfer into Cells in Culture and in vivo: Polyethylenimine.* Proc. Natl. Acad. Sci. USA, 1995. **92**: p. 7297-7301.

26. *Manufacturer's documentation. 408727 Polyethylenimine, branched.* [Accessed January 6, 2011]; Sigma-Aldrich. Available from: http://www.sigmaaldrich.com/catalog/ProductDetail.do?N5=SEARCH_CONC AT_PNO%7CBRAND_KEY&N4=408727%7CALDRICH.

27. Aigner, A., *Nonviral in vivo delivery of therapeutic small interfering RNAs.* Curr Opin Mol Ther, 2007. **9**(4): p. 345-52.

28. Burry, R.W. and J.G. Wood, *Contributions of lipids and proteins to the surface charge of membranes. An electron microscopy study with cationized and anionized ferritin.* J Cell Biol, 1979. **82**(3): p. 726-741.

29. Loftsson, T., et al., *Effects of Cyclodextrins on Drug Delivery Through Biological Membranes.* Journal of Pharmaceutical Sciences, 2007. **96**(10): p. 2532-47.

30. Rajewski, R. and V. Stella, *Pharmaceutical applications of cyclodextrins. 2. in vivo drug delivery.* Journal of Pharmaceutical Sciences, 2000. **85**(11): p. 1142-1169.

31. Neufeld, E., et al., *Intracellular Trafficking of Cholesterol Monitored with a Cyclodextrin.* Journal of Biological Chemistry, 1996. **271**: p. 21604-21613.

32. Challa, R., et al., *Cyclodextrins in Drug Delivery: An Updated Review.* AAPS PharmSciTech, 2005. **6**(2): p. E330-57.

33. Frank, D., J. Gray, and R. Weaver, *Cyclodextrin nephrosis in the rat.* American Journal of Pathology, 1976. **83**(2): p. 367-82.

34. Bøe, S., A. Longva, and E. Hovig, *Cyclodextrin-Containing Polymer Delivery System for Light-Directed siRNA Gene Silencing.* Oligonucleotides, 2010. **20**(4): p. 175-182.

35. Gonzales, H., S. Hwang, and M. Davis, *New Class of Polymers for the Delivery of Macromolecular Therapeutics.* Bioconjugate Chem, 1999. **10**: p. 1068-74.

36. Berg, K., et al., *Photochemical Internalization - A Novel Technology for Delivery of Macromolecules into Cytosol.* Cancer Research, 1999(59): p. 1180.

37. Moan, J. and K. Berg, *The photodegradation of porphyrins in cells can be used to estimate the lifetime of singlet oxygen.* Photochem Photobiol, 1991. **53**(4): p. 549-53.

38. *PCI Biotech Holding ASA - Fourth Quarter 2010 and preliminary full year 2010 Report* 2010(Quarterly report).

39. Berg, K., et al., *Site-specific drug delivery by photochemical internalization enhances the antitumor effect of bleomycin.* Clin Cancer Res, 2005. **11**: p. 8476-8485.

40. Marsh, M., *Endocytosis (Frontiers in Molecular Biology).* Frontiers in Molecular Biology, ed. M. Marsh. 2001: OUP Oxford.

41. Sandvig, K., et al., *Clathrin-independent endocytosis: mechanisms and function.* Current Opinion in Cell Biology, 2011. In Press, Corrected Proof.

42. Kornfield, S. and I. Mellman, *The biogenesis of lysosomes.* Annu Rev Cell Biol, 1989. **5**: p. 483-525.

43. Luzio, J., P. Pryor, and N. Bright, *Lysosomes: Fusion and function.* Nature reviews Molecular Cell Biology, 2007. **8**: p. 622-632.

44. Rosales, C., ed. *Molecular Mechanisms of Phagocytosis (Medical Intelligence Unit).* 2006, Springer.

45. Nam, H.Y., et al., *Cellular uptake mechanism and intracellular fate of hydrophobically modified glycol chitosan nanoparticles.* Journal of Controlled Release, 2009. **135**(3): p. 259-267.

46. Moore, B., *A soluble protein characteristic of the nervous system.* Biochem Biophys Res Column, 1965. **19**(6): p. 739-744.

47. Novitskaya, V., et al., *Oligomeric forms of the metastasis-related Mts1 (S100A4) protein stimulate neuronal differentiation in cultures of hippocampal neurons.* J Biol Chem, 2000. **275**(52): p. 41278-86.

48. Malashkevich, V., et al., *Structure of Ca2+-bound S100A4 and its interaction with peptides derived from nonmuscle myosin-IIA.* Biochemistry, 2008. **47**: p. 5111-5126.

49. Boye, K. and G. Mælandsmo, *S100A4 and metastasis - a small actor playing many roles.* American Journal of Pathology, 2010. **176**(2).

50. Davies, B., et al., *Induction of the metastatic phenotype by transfection of a benign rat mammary epithelial cell line with the gene for p9Ka, a rat calcium-binding protein, but not with the oncogene EJ-ras-1.* Oncogene, 1993. **8**: p. 999-1008.

51. Helfman, D., et al., *The metastasis associated protein S100A4: role in tumour progression and metastasis.* British journal of cancer, 2005. **92**: p. 1955-1958.

52. Boye, K., et al., *Nuclear S100A4 is a novel prognostic marker in colorectal cancer.* Eur J Cancer, 2010. **46**(16): p. 2919-25.

53. Nakamura, N. and K. Takenaga, *Hypomethylation of the metastasis-associated S100A4 gene correlates with gene activation in human colon adenocarcinoma cell lines.* Clin Exp Metastasis, 1998. **16**(5): p. 471-479.

54. Li, C., F. Zhang, and Y. Wang, *S100A proteins in the pathogenesis of experimental corneal neovascularization.* Molecular Vision, 2010. **16**: p. 2225-2235.

55. Ma, X., et al., *Small interfering RNA-directed knockdown of S100A4 decreases proliferation and invasiveness of osteosarcoma cells.* Cancer Letters, 2010. **299**(2): p. 171-181.

56. Fodstad, Ø., et al., *Characteristics of a cell line established from a patient with multiple osteosarcoma, appearing 13 years after treatment for bilateral retinoblastoma.* Int J Cancer, 1986: p. 33-40.

57. Fodstad, Ø., et al., *A new experimental metastasis model in athymic nude mice, the human malignant melanoma LOX.* Int J Cancer, 1988(41(3)): p. 442-449.

58. Lebrun, P., *An Introduction to Cryogenics.* European Organization of Nuclear Research, CERN, 2007(Departmental report).

59. Yokoyama, W., *Cryopreservation of Cells.* Current Protocols in Immunology, 2001: p. A.3G.1–A.3G.3.

60. *Product Information: VenorGeM Mycoplasma Detection Kit, PCR-based. Catalog Number MP0025.* Sigma-Aldrich.

61. *Zetasizer Nano Series User Manual.* 2004(1.1). Malvern Biosciences.

62. Cram, S., *Flow Cytometry, an overview.* Methods in cell science, 2002. **24**.

63. Strand, M., *Establishment of a test system for multiparameter analysis of intracellular signal pathways by the use of flow cytometry.*, in *Institute of Molecular Bioscience.* 2005, University of Oslo.

64. Shapiro, H., *Practical Flow Cytometry.* 4 ed. 2003: John Wiley and sons.

65. *BD Fluorescence Spectrum Viewer - A Multicolor Tool.* BD Biosciences. [cited 2010 dec. 6]; Available from: http://www.bdbiosciences.com/research/multicolor/spectrum_viewer.

66. *Universal Probe Library.* Roche. [cited 2011 January]; Available from: https://www.roche-applied-science.com/sis/rtpcr/upl/index.jsp?id=UP030000.

67. *Primer-BLAST.* NCBI. [cited 2011 January]; Available from: http://www.ncbi.nlm.nih.gov/tools/primer-blast/.

68. Hyndman, D. and M. Mitsuhashi, *PCR Primer Design*, in *PCR Protocols*, J. Bartlett and D. Stirling, Editors. 2003, Humana Press: Costa Mesa, CA, USA. p. 81-8.

69. *Integrated DNA Technologies SciTools OligoAnalyzer.* IDT. 2010 [cited 2011 January]; 3.1:[Available from: http://eu.idtdna.com/analyzer/Applications/OligoAnalyzer.

70. *Illumina® TotalPrep™-96 RNA Amplification Kit (Part Number 4393543) Protocol.* Supplied with microarray results, 2009(revision B). Ambion.

71. Schroeder, A., et al., *The RIN: an RNA integrity number for assigning integrity values to RNA measurements.* BMC Molecular Biology, 2006. **7**(3).

72. *Quality control threshold - RNA QC* 2008 [Accessed April 12, 2011]; ArrayStar. Available from: http://www.arraystar.com/supports/support_main.asp?id=174.

73. Dysvik, B. and I. Jonassen, *J-Express: exploring gene expression data using Java.* Bioinformatics, 2001. **17**(4): p. 369-70.

74. Breitling, R., et al., *Rank products: a simple, yet powerful, new method to detect differentially regulated genes in replicated microarray experiments.* FEBS Letters, 2004. **27**(573): p. 83-92.

75. Jeffery, I., D. Higgins, and A. Culhane, *Comparison and evaluation of methods for generating differentially expressed gene lists from microarray data.* BMC Bioinformatics, 2006. **7**(359).

76. Dennis, G., Jr, et al., *DAVID: Database for Annotation, Visualization, and Integrated Discovery.* Genome Biology, 2003. **4**(5): p. P3.

77. Huang, D., B. Sherman, and R. Lempicki, *Systematic and integrative analysis of large gene lists using DAVID Bioinformatics Resources.* Nature Protocols, 2009. **4**(1): p. 44-57.

78. Bradford, M., *A rapid and sensitive method for the quantitation of microgram quantities of protein utilizing the principle of protein-dye binding.* Anal Biochem, 1976. **72**: p. 248-254.

79. Compton, S. and C. Jones, *Mechanism of dye response and interference in the Bradford protein assay.* Analytical Biochemistry, 1985. **151**(2): p. 369-374.

80. Lea, T., *Immunologi og immunologiske teknikker.* 3 ed. 2006, Bergen: Fagbokforlaget.

81. Gould, H. and B. Sutton, *IgE in allergy and asthma today.* Nature Reviews Immunology, 2008. **8**: p. 205-217.

82. Cory, A., et al., *Use of an aqueous soluble tetrazolium/formazan assay for cell growth assays in culture.* Cancer Communications, 1991. **3**(7): p. 207-12.

83. Berridge, M. and A. Tan, *Characterization of the cellular reduction of 3-(4,5-dimethylthiazol-2-yl)-2,5-diphenyltetrazolium bromide (MTT): subcellular localization, substrate dependence, and involvement of mitochondrial electron transport in MTT reduction.* Arch Biochem Biophys., 1993. **303**(2): p. 474-482.

84. *CellTiter 96® AQueous One Solution - Instructions for use of products G3580, G3581 and G3582.* 2009: Promega, Madison, USA.

85. Sahay, G., D. Alakhova, and A. Kabanov, *Endocytosis of nanomedicines.* Journal of Controlled Release, 2010. **145**(3): p. 182-195.

86. Thyberg, J., U. Hedin, and K. Stenseth, *Endocytic pathways and time sequence of lysosomal transfer of macromolecules in cultured mouse peritoneal macrophages. Double-labeling experiments with horseradish peroxidase and ferritin.* Cell Tissue Res, 1985. **241**(2): p. 299-303.

87. Walker, M.S. and T.A. Hughes, *Messenger RNA expression profiling using DNA microarray technology: Diagnostic tool, scientific analysis or un-interpretable data? (Review).* International Journal of Molecular Medicine, 2008. **21**: p. 13-17.

88. Nygaard, V., et al., *Limitations of mRNA amplification for small-scale cell samples.* BMC Genomics, 2005. **6**(147).

89. Sanchez, D., et al., *Exon-intron structure and evolution of the Lipocalin gene family.* Mol Biol Evol, 2003. **20**(5): p. 775-783.

90. Flower, D., *The lipocalin protein family: structure and function.* Biochem J, 1996. **318**: p. 1-14.

91.   Bratt, T., *Lipocalins and Cancer.* Biochimica et Biophysica Acta, 2000. **1482**:
        p. 318-326.
92.   *Epididymal-specific lipocalin-12 precursor -Homo Sapiens (Human)*. UniProt.
        [Accessed April 4. 2011]; Available from:
        http://www.uniprot.org/uniprot/Q6JVE5.
93.   Peng, Y., et al., *Conformational and biochemical characterization of a rat
        epididymis-specific lipocalin 12 expressed in Escherichia coli.* Biochimica et
        Biophysica Acta, 2010. **1804**(11): p. 2102-2110.
94.   Ibaragi S, et al., *Induction of MMP-13 Expression in Bone-metastasizing
        Cancer Cells by Type I Collagen through Integrin α1β1 and α2β1-p38 MAPK
        Signaling.* Anticancer Research, 2011. **31**(4): p. 1307-13.

Appendix A

C$_t$-values for S100A4

C$_t$-tables for qPCR quantitation of S100A4. For each replicate sample, two measurements were done.

Table A1: C$_t$-values for quantitation of S100A4 in OHS cells. a) Data used for creating the graph shown in figure 3.2b. Fold change is relative to the sample with the highest C$_t$ value. Missing values indicate no deviation. Samples also used in microarray expression profiling are marked with *.

Transfection	Replicate no.	s100a4			
		Mean C$_t$	Ct s.d.	Relative expr.	Expression s.d.
	1*	18.60	0.14	1.32	0.43
	2*	18.25	0.07	3.42	1.32
EGFP 1 µg	3	18.70	-	1.00	0.32
	1*	9.90	0.14	337.79	98.30
	2*	13.55	0.35	34.90	11.28
1µg	3	10.35	0.92	309.76	204.82
	1	8.90	0.28	539.32	121.13
	2	9.15	0.07	430.54	48.35
2µg	3	9.30	-	388.02	28.53
	1*	8.30	-	876.13	194.43
	2*	8.85	0.21	619.52	128.82
3µg	3	8.45	0.07	939.01	79.72

Table A2: Ct-values for quantitation of S100A4 in LOX cells. a) Data used for creating the graph shown in figure 3.2a. Fold change is relative to the sample with the highest C_t value. Missing values indicate no deviation. b) C_t data for samples used in microarray experiment.

Transfection	Replicate no.	s100a4			
		Mean C_t	Ct s.d.	Relative expr.	Expression s.d.
Untransf.	1	18.25	0.07	2.22	0.22
	2**	18.80	0.42	1.00	0.45
	3	19.80	0.14	1.00	0.16
1µg	1	9.90	0.42	711.64	232.67
	2	9.85	0.21	652.58	97.28
	3	10.20	0.28	817.46	183.61
2µg	1	9.15	0.35	1196.83	329.23
	2	9.15	0.21	1327.96	215.87
	3	8.90	0.00	1305.15	172.24
3µg	1	9.00	0.14	1845.76	303.43
	2	8.75	0.07	1722.16	94.37
	3	8.40	0.14	1814.05	226.68

a)

**) data based on one measurement.

Transfection	Replicate no.	s100a4			
		mean C_t	Ct s.d.	Relative expr.	Expression s.d.
EGFP 1 µg	1***	13.80	0.71	47.67	25.16
	2	17.05	0.35	4.59	2.74
1 µg	1	10.75	0.78	265.03	154.93
	2	10.40	0.42	415.87	243.11
3 µg	1	9.80	2.40	630.35	1071.24
	2	9.75	2.19	512.00	780.46

b) ***) Sample excluded from microarray analysis

Appendix B

C$_t$-values for candidate genes

Table B1: C$_t$-values for quantitation of candidate genes CT10, Col1a2, ADAM15, LCN12, and SNORA71c a) in LOX and b) OHS cells, used for creating the graphs shown in figure 3.5. Fold change is relative to the sample with the highest C$_t$ value. Missing values indicate no deviation.

Transfection	Date	CT10 Mean C$_t$	Ct s.d.	Relative Expr.	Expr. s.d.	Col1a2 Mean C$_t$	Ct s.d.	Relative Expr.	Expr. s.d.	ADAM15 Mean C$_t$	Ct s.d.	Relative Expr.	Expr. s.d.
Untransf.	15.02.2010	24.75	1.20	2.83	2.80	33.75	1.20	4.29	4.25	25.20	0.71	1.68	1.22
	28.02.2010	25.00	0.28	1.57	0.70	33.70	0.00	1.83	0.74	24.75	0.35	2.30	1.09
	04.11.2010	25.10	2.55	1.00	1.84	32.15	0.78	1.57	1.18	24.55	0.64	2.14	1.46
1µg	15.02.2010	27.70	0.57	3.25	3.03	36.10	0.14	7.46	6.36	27.10	0.99	4.00	4.36
	28.02.2010	24.75	0.35	1.00	0.31	33.60	0.99	1.05	0.75	25.05	0.35	1.00	0.31
	04.11.2010	23.70	1.56	1.93	2.19	31.20	1.27	2.22	2.10	24.75	1.20	1.37	1.23
3µg	15.02.2010	27.65	1.77	1.00	1.59	37.25	3.46	1.00	2.61	27.35	0.49	1.00	1.07
	28.02.2010	23.75	0.21	1.77	0.29	33.50	0.57	1.00	0.40	24.30	0.42	1.49	0.45
	04.11.2010	24.15	0.49	1.41	0.54	32.35	0.07	1.00	0.18	25.20	0.28	1.00	0.26

Transfection	Date	LCN12 Mean C$_t$	Ct s.d.	Relative Expr.	Expr. s.d.	SNORA71c Mean C$_t$	Ct s.d.	Relative Expr.	Expr. s.d.
Untransf.	15.02.2010					24.35	2.19	1.68	2.71
	28.02.2010	35.70	0.00	3.19	1.29	23.15	0.49	4.14	2.20
	04.11.2010	35.60	0.00	2.00	1.04	24.50	1.27	1.87	1.91
1µg	15.02.2010					25.75	1.77	5.66	8.42
	28.02.2010	35.45	0.49	2.03	0.79	24.30	0.28	1.00	0.27
	04.11.2010	36.15	0.64	1.00	0.56	24.95	1.48	1.00	1.09
3µg	15.02.2010					26.50	2.12	1.00	1.79
	28.02.2010	36.30	1.27	1.00	0.89	23.10	0.28	2.03	0.43
	04.11.2010	36.10	0.42	1.04	0.35	24.95	0.35	1.00	0.30

a) LOX cells

Transfection	Date	CT10 Mean C$_t$	Ct s.d.	Relative Expr.	Expr. s.d.	Col1a2 Mean C$_t$	Ct s.d.	Relative Expr.	Expr. s.d.	ADAM15 Mean C$_t$	Ct s.d.	Relative Expr.	Expr. s.d.
Untransf.	04.03.2011	27.45	1.202	2.55	3.004	22.45	0.636	1.57	1.479	24.45	0.778	1.46	1.453
	21.03.2011	27.65	1.909	1.00	1.409	22.95	1.909188	1.00	1.40864	24.80	1.6971	1.00	1.2715
1µg	04.03.2011	24.15	0.636	9.85	5.222	19.70	0.566	4.14	2.030	22.05	0.495	3.03	1.370
	21.03.2011	24.10	0.566	8.00	3.161	19.80	0.424264	6.06	1.80755	21.45	0.2121	6.96	1.07943
3µg	04.03.2011	29.75	1.061	1.00	0.833	24.05	0.919	1.00	0.748	25.95	0.778	1.00	0.667
	21.03.2011	27.10	0.849	2.07	1.346	21.80	0.565685	3.14	1.50711	24.20	0.8485	2.14	1.3938

Transfection	Date	LCN12 Mean C$_t$	Ct s.d.	Relative Expr.	Expr. s.d.	SNORA71c Mean C$_t$	Ct s.d.	Relative Expr.	Expr. s.d.
Untransf.	04.03.2011	36.40	0.1414	7.46	6.26226	25.50	0.989949	1.52	1.63606
	21.03.2011	36.95	0.0707	5.10	2.47368	25.90	1.273	1.00	1.006
1µg	04.03.2011	37.95	0.495	1.00	0.45188	23.70	0	2.07	0.6089
	21.03.2011	38.40	0	1.27	0.06247	22.35	0.495	8.00	2.773
3µg	04.03.2011	Undetected				27.05	0.494975	1.00	0.52101
	21.03.2011	39.80	0	1.00	0.27726	25.40	0.566	2.00	0.960

b) OHS cells

Appendix C

Primer sequences

Primers used in the qPCR reactions. Melting temperature (T_m) is calculated from the percentage of G and C nucleotides in the primer sequence.

Gene symbol	Primer direction	Sequence (5' to 3')	Tm (^{o}C)	Transcript length
S100A4	Forward	AAGTTCAAGCTCAACAAGTCAGAAC	49	79
	Reverse	CATCTGTCCTTTTCCCCAAGA	47	
TBP	Forward	GCCCGAAACGCCGAATAT	56	64
	Reverse	CGTGGCTCTCTTATCCTCATGA	56	
RPLPO	Forward	CGCTGCTGAACATGCTCAAC	57	64
	Reverse	TCGAACACCTGCTGGATGAC	57	
CT10	Forward	CGCGTCTCCCACTACATCA	60	95
	Reverse	AGTCTGGAGGGGCTCACC	60	
COL1A2	Forward	CTGGAGAGGCTGGTACTGCT	59	62
	Reverse	AGCACCAAGAAGACCCTGAG	59	
ADAM15	Forward	GGCATGGCCATTCAGAAC	60	77
	Reverse	AGGATGCTGGTGGAGTGGT	60	
LCN12	Forward	CAACATCGTCTTCCCAGATG	59	73
	Reverse	CAGGAGCTGCTTCATCCTTC	60	
SNORA71c	Forward	CCCCTGCATTCGAAAGTG	60	80
	Reverse	AAGTGCTCTCGGCAGTTCC	60	
LOC646496	Forward	GTGCGCACCGATGGAAGCCT	63	66
	Reverse	TGCGCTCGGCTTCTCCCGTA	64	

Appendix D

Particle size measurements

Graphical representation of sizes of transfection particles. a) 1 µg mRNA. Main peak average: 377 nm. b) 2 µg mRNA. Main peak average: 534 nm. c) 3µg mRNA. Main peak average: 540 nm. Two peaks of differently sized particles are observed in each measurement; one large peak, and a smaller peak of smaller sized particles. The smaller peaks are presumed to correspond to uncomplexed or partly complexed constituents. Figures made in ZetaSizer software.

a)

b)

c)
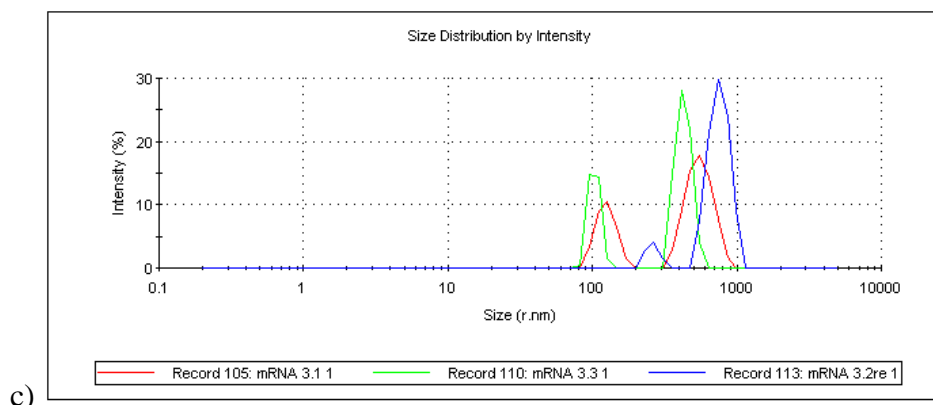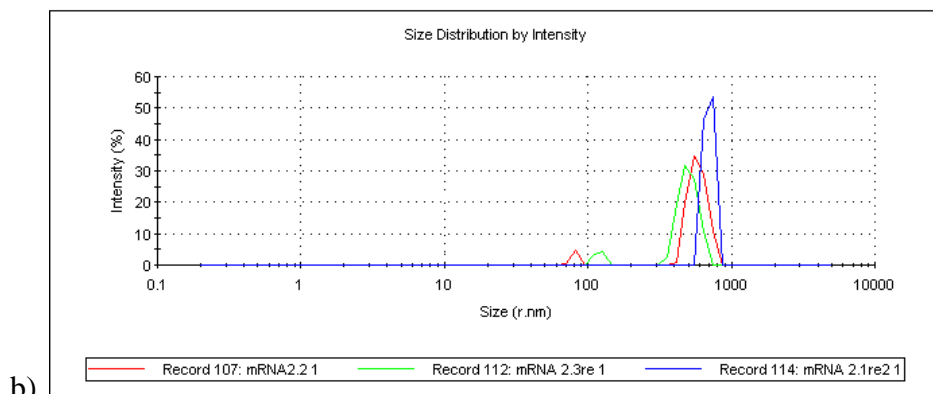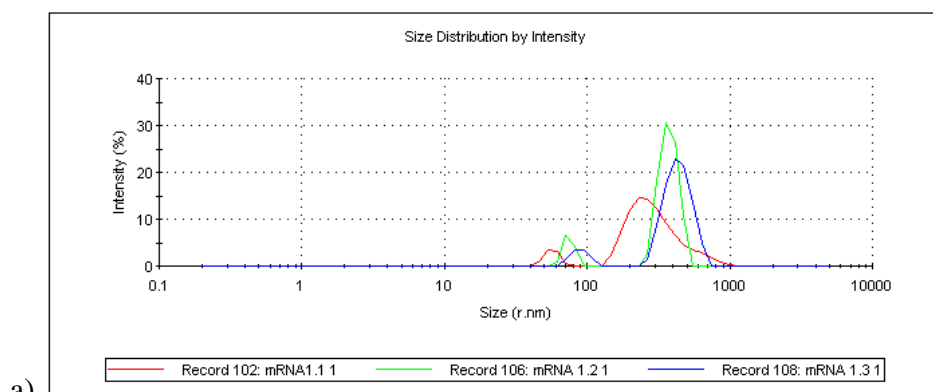
Appendix E

Buffers and solutions used in the study

Table E1: Growth medium supplements

Supplement	Concentration	Per 500 ml RPMI 1640
Fetal calf serum	10%	50 ml
glutaMAX	2 mM	5.5 ml of 200 mM stock

Table E2: Constitutents of freeze medium

Constituent	Volume
RPMI 1640 w/serum, L-glutamine	16.5 ml
Fetal calf serum	1.5 ml
DMSO (sterile)	2 ml

Table E3: Constituents of qPCR master mixes. Listed volumes were multiplied with the number of samples plus two (negative control plus a surplus to allow for pipetting error).

Reagent	Volume per sample in assay
iQ SYBR Green Supermix	30 µl
Primer reverse, 10 pmol/µl	1.8 µl
Primer forward, 10 pmol/µl	1.8 µl
Sterile H_2O	16.4 µl
Total	50 µl

Table E4: Constituents of acrylamide electrophoresis gels. After addition of TEMED, the gel is solid within 10-15 minutes.

Reagent	Volume	Producer
TAE 1x	9.6 ml	Invitrogen
Acrylamide 40%	2.25 ml	Bio-Rad
Ammonium persulfate (APS) 20%, freshly thawed (less than 4 weeks since thawed)	90 µl	Bio-Rad
TEMED (1,2-bis[dimethylamino]- ethane)	20 µl	Bio-Rad

Table E5: Constituents of lysis buffer.

Lysis buffer:		For 50 ml:	
Compound	**Concentration**	**Compound**	**Volume**
NaCl	150 mM	5 M NaCl	1.5 ml
Tris pH 7.5	50 mM	0.5 M Tris pH 7.5	5 ml
Nonidet P40	0.10%	Nonidet P40	50 μl
Double distilled H_2O		Double-distilled H_2O	to 50 ml

The solution was stored at $4^{o}C$.

Protease inhibitors PMSF, leupeptin, pepstatin, and aprotinin (all 2 mM; Sigma-Aldrich) were added to the lysis buffer before use; 10 μl of each to 1 ml of lysis buffer.

Table E6: Preparation of protein samples for gel electrophoresis.

Compound	**Volume (μl)**	**Producer**
Sample	X	
de-ionized H2O	to 6.5	
NuPage LDS sample buffer (4x)	2.5	Bio-Rad
NuPage Reducing Agent	1	Bio-Rad
Total	10	

Directly after the addition of reducing agent, samples were heated at $70^{o}C$ on a heat block for 10 minutes.

Table E7: Contents of 0.25% TBST buffer:

Compound	**Volume**
Tris pH 7.5 1M	20 ml
NaCl 5M	100 ml
Tween 20	2.5 ml
double destilled H2O	to 1 l